Journal of Sound and Vibration (1998) **217**(4), 691–736
Article No. sv981781

ANALYSIS OF NON-LINEAR DYNAMICS AND BIFURCATIONS OF A DOUBLE PENDULUM

P. Yu and Q. Bi*

Department of Applied Mathematics, University of Western Ontario, London, Ontario, Canada R6A 5B7

(*Received* 15 *January* 1998, *and in final form* 20 *May* 1998)

In this paper, the dynamic behaviour of a double pendulum system in the vicinity of several compound critical points is explored through both analytical and numerical approaches. Four types of critical points are considered, which are characterized by a double zero eigenvalue, a simple zero and a pair of pure imaginary eigenvalues, and two pairs of pure imaginary eigenvalues including resonant and non-resonant cases. With the aid of normal form theory, the explicit expressions for the critical bifurcation lines leading to incipient and secondary bifurcations are obtained. Possible bifurcations leading to 2-D and 3-D tori are also investigated. Closed form stability conditions of the bifurcation solutions are presented. A time integration scheme is used to find the numerical solutions for these bifurcation cases, which agree with the analytic results. Finally, numerical simulation is also applied to obtain double-period cascading bifurcations leading to chaos.

1. INTRODUCTION

A non-linear autonomous system may exhibit complex dynamic behaviour in the vicinity of a *compound* critical point. According to the structure of the Jacobian of the system evaluated at the critical point, the systems may be classified, in general, as codimension one, codimension two, etc. [1]. There are three codimension two systems characterized by (1) a double zero eigenvalue, (2) a simple zero and a pair of pure imaginary eigenvalues, and (3) two pairs of pure imaginary eigenvalues. It has been shown that not only *static* bifurcations but also *dynamic* (periodic) bifurcations may occur even in the vicinity of a double zero critical point (the lowest order compound critical point) of a non-linear autonomous system [1, 2]. (In this paper, a dynamic bifurcation means that for a given set of system parameters a motion bifurcates from an equilibrium or another movement.) Systems characterized by a critical point with a simple zero and a pair of pure imaginary eigenvalues have also been considered by many researchers (e.g., see references [1, 3, 4]). In addition to static and dynamic bifurcations, such a system may have the interaction between the static and dynamic modes leading to two-dimensional (2-D) tori. When a critical point of

0022–460X/98/440691 + 46 $30.00/0

the system is characterized by two pairs of pure imaginary eigenvalues, the system may exhibit periodic solutions as well as more complex phenomena such as quasi-periodic motions on 2-D or 3-D tori (for example, see references [1, 5, 6]).

Many physical or engineering systems are able to exhibit complex dynamical behaviour in the vicinity of a codimension two compound critical point. A double pendulum system may be the simplest one of such systems. Many researchers have studied the double pendulum to show bifurcation and stability properties of the system in the vicinity of a critical point. For example, Mandadi and Huseyin [7] considered the double pendulum system for various compound critical points including a double zero, a triple zero, and a double zero and a pair of pure imaginary eigenvalues, and derived explicit approximate solutions by using a perturbation technique [8]. However, only *divergence* (static) bifurcations were studied in their paper. Later, Scheidl *et al*. [9] applied an averaging method to obtain the general formulae for both stationary and periodic solutions bifurcating from a critical point characterized by a simple zero and a pair of pure imaginary eigenvalues. However, possible secondary bifurcations and sequence of bifurcations leading to quasi-periodic motions on 2-D tori were not discussed. When the double pendulum system is characterized by a critical point with two pairs of pure imaginary eigenvalues, the resonant and non-resonant behaviour are usually concerned (for example, see reference [10]). However, instead of the double pendulum, many researchers used models of coupled oscillators to study, in particular, bifurcations into invariant tori (e.g., see references [11–19]). It has been noticed that most work done related to a double pendulum has been focused on analytic study and not many numerical results have been published.

In this paper, both analytical and numerical approaches are employed to consider the double pendulum system. All the three types of compound critical points will be studied in detail. Normal form theory, bifurcation and stability theory are used to find closed form solutions for equilibria, periodic and quasi-periodic motions. Stability conditions for these bifurcation solutions are obtained explicitly. Moreover, critical boundaries along which incipient, secondary and tertiary bifurcations leading to 2-D and 3-D tori are also derived. All the analytic results are obtained by using a symbolic computation language Maple. Furthermore, a time integration scheme is used to find all the numerical solutions corresponding to the analytic study. It is shown that all numerical solutions agree with the analytic prediction, at least qualitatively.

In the next section, the mathematical model for the double pendulum system is derived in terms of a set of first-order differential equations. Sections 3, 4 and 5 are devoted to the studies on the dynamical behaviour of the system in the vicinity of the critical points: a double zero, a simple zero and a pair of pure imaginary eigenvalues, and two pairs of pure imaginary eigenvalues, respectively. In section 6, 1:1 primary resonance is considered to find phase-locked periodic solutions. Section 7 presents the numerical results showing that the double pendulum exhibits period-doubling cascading bifurcations leading to chaos. Finally, conclusions are drawn in section 8.

2. PROBLEM STATEMENT

The double pendulum system shown in Figure 1 consists of two rigid weightless links of equal length l which carry two concentrated masses $2m$ and m, respectively. A follower force P_1 and a constant directional force (vertical) P_2 are applied to this system.

The system energy for the three linear springs h_1, h_2 and h_3 is assumed to be given by [7]

$$V = \tfrac{1}{2}[(h_1 + h_2 + h_3 l^2)\theta_1^2 + 2(h_3 l^2 - h_2)\theta_1\theta_2 + (h_2 + h_3 l^2)\theta_2^2] - \tfrac{1}{6}h_3 l^2(\theta_1 + \theta_2)(\theta_1^3 + \theta_2^3), \quad (1)$$

where θ_1 and θ_2 are generalized co-ordinates which specify the configuration of the system completely.

The kinetic energy T of the system is expressed by

$$T = \frac{ml^2}{2\Omega^2}[3\dot{\theta}_1^2 + \dot{\theta}_2^2 + 2\dot{\theta}_1\dot{\theta}_2 \cos(\theta_1 - \theta_2)], \quad (2)$$

where Ω is an arbitrary value rendering the time variable non-dimensional, and the overdot denotes differentiation with respect to the non-dimensional time variable τ and $\tau = \Omega t$.

The components of the generalized forces corresponding to the generalized co-ordinates θ_1 and θ_2 may be written as

$$Q_1 = P_1 l \sin(\theta_1 - \theta_2) + 2P_2 l \sin\theta_2, \qquad Q_2 = P_2 l \sin\theta_2, \quad (3)$$

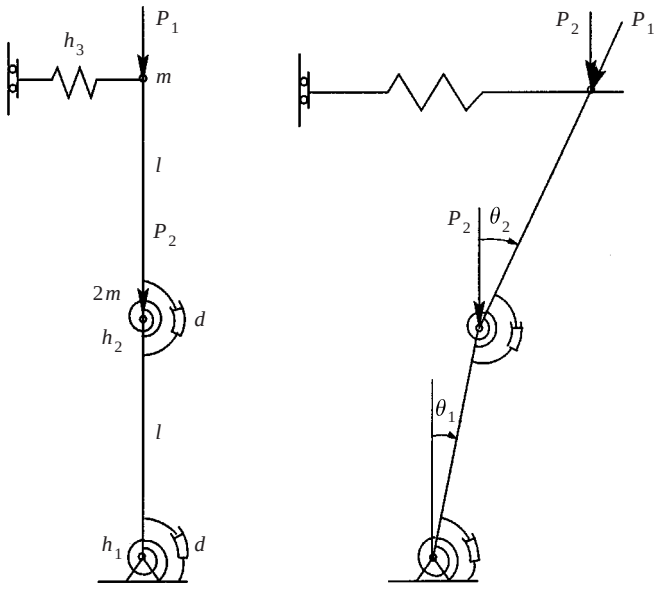

Figure 1. A double pendulum system.

and the damping can be expressed by

$$D = \tfrac{1}{2}[d_1\dot{\theta}_1^2 + d_2(\dot{\theta}_1 - \dot{\theta}_2)^2] + \tfrac{1}{4}[d_3\dot{\theta}_1^4 + d_4(\dot{\theta}_1 - \dot{\theta}_2)^4], \tag{4}$$

where d_1, d_2 represents the linear parts and d_3, d_4 describe the non-linear parts, respectively.

With the aid of the *Langrangian equations*, in addition, choosing the state variables

$$z_1 = \theta_1, \qquad z_2 = \dot{\theta}_1, \qquad z_3 = \theta_2 \quad \text{and} \quad z_4 = \dot{\theta}_2, \tag{5}$$

and rescaling the coefficients to be dimensionless coefficients as

$$f_1 = \frac{h_1\Omega^2}{ml^2}, \qquad f_2 = \frac{h_2\Omega^2}{ml^2}, \qquad f_3 = \frac{h_3\Omega^2}{m}, \qquad f_4 = \frac{P_1\Omega^2}{ml}, \qquad f_5 = \frac{P_2\Omega^2}{ml},$$
$$f_6 = \frac{d_3\Omega^4}{ml^2}, \qquad f_7 = \frac{d_4\Omega^4}{ml^2}, \qquad \eta_1 = \frac{d_1\Omega^2}{ml^2}, \qquad \eta_2 = \frac{d_2\Omega^2}{ml^2}, \tag{6}$$

one can derive a set of first order differential equations up to third order terms as follows:

$$\frac{\mathrm{d}z_1}{\mathrm{d}\tau} = z_2,$$

$$\begin{aligned}\frac{\mathrm{d}z_2}{\mathrm{d}\tau} = {} & (-\tfrac{1}{2}f_1 - f_2 + \tfrac{1}{2}f_4 + f_5)z_1 - (\tfrac{1}{2}\eta_1 + \eta_2)z_2 + (f_2 - \tfrac{1}{2}f_4 - \tfrac{1}{2}f_5)z_3 + \eta_2 z_4 \\ & + (\tfrac{1}{4}f_1 + \tfrac{3}{4}f_2 - \tfrac{1}{3}f_4 - \tfrac{2}{3}f_5)z_1^3 + (-\tfrac{3}{4}f_2 - \tfrac{1}{2}f_3 + \tfrac{1}{3}f_4 + \tfrac{7}{12}f_5)z_3^3 + f_7 z_4^3 \\ & - (\tfrac{1}{2}f_6 + f_7)z_2^3 + (\tfrac{3}{4}\eta_2 + \tfrac{1}{4}\eta_1)z_1^2 z_2 - (\tfrac{1}{2}f_1 + \tfrac{9}{4}f_2 - \tfrac{1}{2}f_3 - f_4 - \tfrac{3}{2}f_5)z_1^2 z_3 \\ & - \tfrac{3}{4}\eta_2 z_1^2 z_4 - \tfrac{1}{2}z_1 z_2^2 + \tfrac{1}{2}z_2^2 z_3 + 3f_7 z_2^2 z_4 + (\tfrac{1}{4}f_1 + \tfrac{9}{4}f_2 - f_4 - \tfrac{3}{2}f_5)z_1 z_3^2 \\ & + (\tfrac{1}{4}\eta_1 + \tfrac{3}{4}\eta_2)z_2 z_3^2 - \tfrac{3}{4}\eta_2 z_3^2 z_4 - \tfrac{1}{2}z_1 z_4^2 - 3f_7 z_2 z_4^2 + \tfrac{1}{2}z_3 z_4^2 \\ & - (\tfrac{1}{2}\eta_1 + \tfrac{3}{2}\eta_2)z_1 z_2 z_3 + \tfrac{3}{2}\eta_2 z_1 z_3 z_4,\end{aligned}$$

$$\frac{\mathrm{d}z_3}{\mathrm{d}\tau} = z_4,$$

$$\begin{aligned}\frac{\mathrm{d}z_4}{\mathrm{d}\tau} = {} & (\tfrac{1}{2}f_1 + 2f_2 - f_3 - \tfrac{1}{2}f_4 - f_5)z_1 + (\tfrac{1}{2}\eta_1 + 2\eta_2)z_2 + (-2f_2 - f_3 + \tfrac{1}{2}f_4 + \tfrac{3}{2}f_5)z_3 \\ & - 2\eta_2 z_4 - (\tfrac{1}{2}f_1 + \tfrac{5}{4}f_2 - \tfrac{1}{6}f_3 - \tfrac{7}{12}f_4 - \tfrac{7}{6}f_5)z_1^3 + (\tfrac{5}{4}f_2 + \tfrac{7}{6}f_3 - \tfrac{7}{12}f_4 - f_5)z_3^3 \\ & + (\tfrac{1}{2}f_6 + 2f_7)z_2^3 - 2f_7 z_4^3 - (\tfrac{1}{2}\eta_1 + \tfrac{5}{4}\eta_2)z_1^2 z_2 + (f_1 + \tfrac{15}{4}f_2 - \tfrac{1}{2}f_3 - \tfrac{7}{4}f_4 - \tfrac{11}{4}f_5)z_1^2 z_3 \\ & + \tfrac{5}{4}\eta_2 z_1^2 z_4 + \tfrac{3}{2}z_1 z_2^2 - (\tfrac{1}{2}f_1 + \tfrac{15}{4}f_2 - \tfrac{1}{2}f_3 - \tfrac{7}{4}f_4 - \tfrac{5}{2}f_5)z_1 z_3^2 - \tfrac{3}{2}z_2^2 z_3 \\ & - 6f_7 z_2^2 z_4 - (\tfrac{1}{2}\eta_1 + \tfrac{5}{4}\eta_2)z_2 z_3^2 + \tfrac{5}{4}\eta_2 z_3^2 z_4 + \tfrac{1}{2}z_1 z_4^2 + 6f_7 z_2 z_4^2 - \tfrac{1}{2}z_3 z_4^2 \\ & + (\eta_1 + \tfrac{5}{2}\eta_2)z_1 z_2 z_3 - \tfrac{5}{2}\eta_2 z_1 z_3 z_4,\end{aligned} \tag{7}$$

where $f_i \geqslant 0$ ($i = 1, 2, 3$) due to physical conditions, and f_4 and f_5 (or P_1 and P_2) are used to indicate the system parameters for the first two bifurcation cases considered in sections 3 and 4, while η_1 and η_2 for the remaining three bifurcation cases are studied in sections 5, 6, and 7.

The Jacobian matrix of equation (7) evaluated at an arbitrary point on the initial equilibrium solution $z_i = 0$ takes the form

$$J = \begin{bmatrix} 0 & 1 & 0 & 0 \\ -\frac{1}{2}f_1 - f_2 + \frac{1}{2}f_4 + f_5 & -\eta_2 - \frac{1}{2}\eta_1 & f_2 - \frac{1}{2}f_4 - \frac{1}{2}f_5 & \eta_2 \\ 0 & 0 & 0 & 1 \\ \frac{1}{2}f_1 + 2f_2 - f_3 - \frac{1}{2}f_4 - f_5 & 2\eta_2 + \frac{1}{2}\eta_1 & -2f_2 - f_3 + \frac{1}{2}f_4 + \frac{3}{2}f_5 & -2\eta_2 \end{bmatrix}, \tag{8}$$

from which one may obtain the characteristic polynomial

$$P(\lambda) = \lambda^4 + a_1\lambda^3 + a_2\lambda^2 + a_3\lambda + a_4, \tag{9}$$

where

$$\begin{aligned} a_1 &= \frac{1}{2}\eta_1 + 3\eta_2, \\ a_2 &= 3f_2 + \frac{1}{2}\eta_1\eta_2 + \frac{1}{2}f_1 - f_4 - \frac{5}{2}f_5 + f_3, \\ a_3 &= 2\eta_2 f_3 - \frac{1}{2}\eta_1 f_5 + \frac{1}{2}f_1\eta_2 + \frac{1}{2}\eta_1 f_3 + \frac{1}{2}\eta_1 f_2 - \frac{3}{2}\eta_2 f_5, \\ a_4 &= 2f_2 f_3 - \frac{3}{2}f_2 f_5 + \frac{1}{2}f_1 f_2 + \frac{1}{2}f_1 f_3 - \frac{1}{2}f_1 f_5 + \frac{1}{2}f_4 f_5 - \frac{3}{2}f_5 f_3 + f_5^2 - f_4 f_3. \end{aligned} \tag{10}$$

Using the *Hurwitz criterion* [20], one may show that when

$$a_1 > 0, \qquad a_2 > 0, \qquad a_4 > 0 \quad \text{and} \quad a_3(a_1 a_2 - a_3) - a_4 a_1^2 > 0, \tag{11}$$

the initial equilibrium solution $z_i = 0$ is stable. It should be noted that the conditions given in equation (11) imply $a_3 > 0$, which is of course as expected. Now let us consider the violations of the four conditions given in equation (11) leading to codimension one bifurcations occurring from the stable equilibrium $z_i = 0$. It is not difficult to find from equations (11) that the condition which may be first violated is either $a_4 > 0$ or $a_3(a_1 a_2 - a_3) - a_4 a_1^2 > 0$, since if a_1 crosses zero first (i.e., positive a_1 becomes zero) while a_2, a_3 and a_4 are still positive, then the fourth condition becomes $-a_3^2 < 0$, which had already crossed zero. Similarly, if a_2 crosses zero first, but a_1, a_2 and a_4 are still positive, then the fourth condition becomes $-a_3^2 - a_4 a_1^2 < 0$, which again already violates the stability conditions. Thus, there exist only two types of codimension one bifurcations which may occur from the initial equilibrium: One is a static bifurcation when $a_4 = 0$, which gives a zero eigenvalue at the critical point; the other is a dynamic (Hopf) bifurcation when $a_3(a_1 a_2 - a_3) - a_4 a_1^2 = 0$ under which the characteristic polynomial (9) has one pair of pure imaginary eigenvalues.

Similarly, one can discuss and find the conditions leading to codimension two bifurcations, which are studied in detail in the following sections.

3. A DOUBLE ZERO EIGENVALUE

We start with the simplest case of codimension two bifurcations in which the characteristic polynomial (9) is supposed to have a double zero and two distinct negative eigenvalues

$$\lambda_{1,2} = 0, \quad \lambda_3 = -1, \quad \lambda_4 = -3, \tag{12}$$

which implies that $a_1 = 4$, $a_2 = 3$ and $a_3 = a_4 = 0$. The values of the physical parameters may then be determined from equation (10), and one choice corresponding to the critical point is defined by

$$f_1 = 8, \quad f_2 = 10, \quad f_3 = \frac{32}{11}, \quad f_4 = \frac{134}{11}, \quad f_5 = \frac{100}{11}, \quad f_6 = f_7 = 0, \quad \eta_1 = 2, \quad \eta_2 = 1. \tag{13}$$

Choosing f_4 and f_5 (initially, P_1 and P_2) as the parameters, and then using the parameter transformation

$$f_4 = \frac{134}{11} + \mu_1, \qquad f_5 = \frac{100}{11} + \mu_2, \tag{14}$$

and the state variable transformation

$$\begin{Bmatrix} z_1 \\ z_2 \\ z_3 \\ z_4 \end{Bmatrix} = \begin{bmatrix} 1 & 0 & -1 & -2 \\ 0 & 1 & 1 & 6 \\ \frac{13}{7} & \frac{80}{49} & -\frac{4}{3} & 1 \\ 0 & \frac{13}{7} & \frac{4}{3} & -3 \end{bmatrix} \begin{Bmatrix} x_1 \\ x_2 \\ x_3 \\ x_4 \end{Bmatrix}, \tag{15}$$

one may transform equation (7) into a new system:

$$\frac{\mathrm{d}x_1}{\mathrm{d}\tau} = x_2 + \left(\frac{87}{77}\mu_1 + \frac{1871}{1386}\mu_2\right)x_1 + \left(\frac{899}{1078}\mu_1 + \frac{4211}{485}\mu_2\right)x_2$$

$$-\left(\frac{29}{66}\mu_1 + \frac{67}{297}\mu_2\right)x_3 + \left(\frac{87}{22}\mu_1 + \frac{1469}{198}\mu_2\right)x_4 + Nf_1,$$

$$\frac{\mathrm{d}x_2}{\mathrm{d}\tau} = -\left(\frac{6}{11}\mu_1 + \frac{10}{33}\mu_2\right)x_1 - \left(\frac{31}{77}\mu_1 + \frac{26}{231}\mu_2\right)x_2$$

$$+\left(\frac{7}{33}\mu_1 - \frac{14}{99}\mu_2\right)x_3 - \left(\frac{21}{11}\mu_1 + \frac{112}{33}\mu_2\right)x_4 + Nf_2,$$

$$\frac{dx_3}{d\tau} = -x_3 + \left(\frac{9}{11}\mu_1 + \frac{213}{154}\mu_2\right)x_1 + \left(\frac{93}{154}\mu_1 + \frac{531}{539}\mu_2\right)x_2$$

$$-\left(\frac{7}{22}\mu_1 + \frac{5}{11}\mu_2\right)x_3 + \left(\frac{63}{22}\mu_1 + \frac{123}{22}\mu_2\right)x_4 + Nf_3,$$

$$\frac{dx_4}{d\tau} = -3x_4 - \left(\frac{9}{77}\mu_1 + \frac{233}{1386}\mu_2\right)x_1 - \left(\frac{93}{1078}\mu_1 + \frac{577}{4851}\mu_2\right)x_2$$

$$+\left(\frac{1}{22}\mu_1 + \frac{13}{297}\mu_2\right)x_3 - \left(\frac{9}{22}\mu_1 + \frac{155}{198}\mu_2\right)x_4 + Nf_4, \tag{16}$$

where the non-linear functions Nf_i are given in Appendix A. The Jacobian matrix of equation (16) evaluated on the initial equilibrium solution $x_i = 0$ at the critical point $\mu_{1c} = \mu_{2c} = 0$ is now in the canonical form

$$J_{(x_i=0)} = \begin{bmatrix} 0 & 1 & 0 & 0 \\ 0 & 0 & 0 & 0 \\ 0 & 0 & -1 & 0 \\ 0 & 0 & 0 & -3 \end{bmatrix}. \tag{17}$$

3.1. BIFURCATION ANALYSIS

The local dynamic behaviour of system (16) is characterized by the critical variables x_1 and x_2. Furthermore, the bifurcation solutions for the non-critical variables x_3 and x_4 may be determined from equation (16) up to leading order terms as

$$x_3 = \left(\frac{9}{11}\mu_1 + \frac{213}{154}\mu_2\right)x_1 + \left(\frac{93}{154}\mu_1 + \frac{531}{539}\mu_2\right)x_2$$

$$+\frac{4769}{539}x_1^3 + \frac{1\,505\,233}{369\,754}x_2^3 + \frac{94\,296}{3773}x_1^2x_2 + \frac{503\,385}{26\,411}x_1x_2^2,$$

$$x_4 = -\left(\frac{3}{77}\mu_1 + \frac{233}{4158}\mu_2\right)x_1 - \left(\frac{31}{1078}\mu_1 + \frac{557}{14\,553}\mu_2\right)x_2$$

$$-\frac{38\,491}{101\,871}x_1^3 - \frac{34\,456\,445}{209\,650\,518}x_2^3 - \frac{69\,448}{64\,827}x_1^2x_2 - \frac{4\,012\,927}{4\,991\,679}x_1x_2^2. \tag{18}$$

Therefore, one may verify that neglecting x_3 and x_4 (i.e., setting $x_3 = x_4 = 0$) in the first two equations of equations (16) does not affect the results of the bifurcation solutions (x_1, x_2) and their stability conditions up to leading order terms. So, in order to consider the bifurcation and stability properties of system (16) in the

vicinity of the critical point c, one only needs to analyze the following simpler two-dimensional system:

$$\frac{dx_1}{d\tau} = x_2 + \left(\frac{87}{77}\mu_1 + \frac{1871}{1386}\mu_2\right)x_1 + \left(\frac{1}{36}\mu_1 + \frac{2}{9}\mu_2\right)x_2 + \frac{330\,733}{33\,957}x_1^3$$

$$+ \frac{275\,353\,739}{69\,883\,506}x_2^3 + \frac{6\,593\,768}{237\,699}x_1^2x_2 + \frac{33\,961\,273}{1\,663\,893}x_1x_2^2,$$

$$\frac{dx_2}{d\tau} = -\left(\frac{6}{11}\mu_1 + \frac{10}{33}\mu_2\right)x_1 - \left(\frac{31}{77}\mu_1 + \frac{26}{231}\mu_2\right)x_2 - \frac{5108}{1617}x_1^3$$

$$- \frac{1\,423\,276}{1\,663\,893}x_2^3 - \frac{103\,856}{11\,319}x_1^2x_2 - \frac{489\,232}{79\,233}x_1x_2^2, \tag{19}$$

corresponding to the Jordan block with a double zero of index one eigenvalue. The reduced system (19) can be easily verified by using the center manifold theory [21, 22].

Now, based on equation (19), the results and formulae obtained previously [2] can be applied here. It is noted that system (19) is a special case listed in the last column of Table 1 of reference [2]. Applying the general formula yields the following results.

The stability conditions for the initial equilibrium solution $x_i = 0$ are described by

$$18\mu_1 + 10\mu_2 > 0 \quad \text{and} \quad 144\mu_1 + 245\mu_2 < 0, \tag{20}$$

which lead to two critical bifurcation lines. One of these is

$$L_1: \quad 18\mu_1 + 10\mu_2 = 0 \qquad (144\mu_1 + 245\mu_2 < 0) \tag{21}$$

along which a static bifurcation solution takes place from the initial equilibrium solution and the solution is expressed by

$$x_1^2 = -\frac{49}{2554}(9\mu_1 + 5\mu_2),$$

$$x_2 = \frac{1}{252\,846}(139\,545\mu_1 - 105\,086\mu_2)x_1. \tag{22}$$

It is noted that this special case is a so called *pitchfork* bifurcation.

On the other hand, the second critical line

$$L_2: \quad 144\mu_1 + 245\mu_2 = 0 \qquad (18\mu_1 + 10\mu_2 > 0), \tag{23}$$

describes a dynamic boundary where the initial equilibrium solution loses its stability and bifurcates into a family of limit cycles. Again from Table 1 of reference [2], one may find the stability condition for the family of limit cycles, given by

$$\gamma_{11} - \gamma_{22} = \frac{32\,411}{1078} > 0, \tag{24}$$

so the family of limit cycles bifurcating from the initial equilibrium is unstable.

The static bifurcation solution (22) becomes unstable on the third critical line, described by

$$L_3: \quad 691\,209\mu_1 + 173\,300\mu_2 = 0 \qquad (18\mu_1 + 33\mu_2 < 0), \tag{25}$$

from which another family of limit cycles—which is usually called *secondary* Hopf bifurcations—occurs. The frequency of this family of limit cycles is

$$\omega_c = \sqrt{-\frac{2}{33}(18\mu_1 + 10\mu_2)} > 0, \tag{26}$$

where $18\mu_1 + 10\mu_2 < 0$ since the secondary Hopf bifurcation solution exists in the region located on the left of the critical line L_1 (see Figure 2). The stability condition for this family of limit cycles can be obtained as follows: first translate system (19) from the initial equilibrium $x_i = 0$ to the static bifurcation solution (22) (which implies that the static bifurcation solution now represents the origin in the new co-ordinate system), and then use the formula given in Table 1 of reference [2] to find that the leading term of $\gamma_{11} - \gamma_{22}$ is given by

$$\gamma_{11} - \gamma_{22} = -\frac{369\,063}{30\,184\omega_c} < 0 \quad (\text{since } \omega_c > 0). \tag{27}$$

Therefore, the secondary Hopf bifurcation solution is stable.

The critical bifurcation lines are illustrated in the parameter space shown in Figure 2, where the numbers given in the brackets denote the slope of the critical

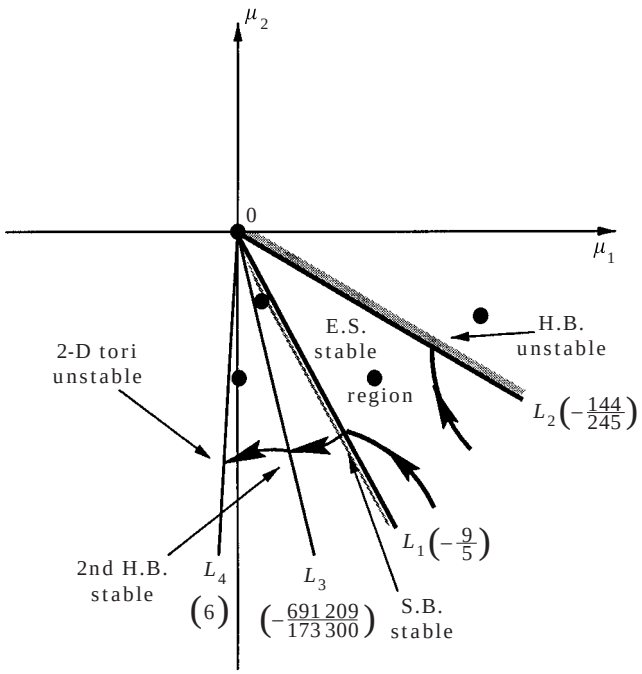

Figure 2. Bifurcation diagram for the case of double-zero eigenvalue.

lines. The notations, E.S., S.B., H.B., 2nd H.B. and 2-D Tori represent initial equilibrium solution, static bifurcation solution, Hopf bifurcation solution, secondary Hopf bifurcation solution and 2-D tori, respectively. The stable region for the E.S. is bounded by the critical lines L_1 and L_2. The S.B. solution branching off the critical line L_1 is stable in the region bounded by the critical lines L_1 and L_3, while the periodic solutions bifurcating from the critical line L_2 is unstable. The 2nd H.B. solution is stable in the region bounded by the critical lines L_3 and L_4, the critical line L_4 is determined by a numerical approach.

3.2. NUMERICAL RESULTS

Numerical results have been obtained by using a time integration scheme—fourth-order Runge–Kutta method. The numerical computation is performed on the basis of the original differential equation (7). Different parameter values of μ_1 and μ_2 are chosen from the different regions shown in Figure 2 to confirm the analytic results obtained in the previous subsection. The black circle dots shown in the parameter space (see Figure 2) indicate these parameter values. For the parameter value $(\mu_1, \mu_2) = (0{\cdot}3, -0{\cdot}1)$, which is located above the critical line L_2, numerical results show that any solution starting from an arbitrary initial point diverges to infinity, indicating that the H.B. solution is unstable, as predicted by the analytic study. When the parameter value is chosen from the stable region of the E.S., say, $(\mu_1, \mu_2) = (0{\cdot}18, -0{\cdot}18)$, a numerical solution starting from an initial point $(z_1, z_2, z_3, z_4) = (0{\cdot}03, 0{\cdot}0, 0{\cdot}03, 0{\cdot}0)$ is obtained, which converges to the origin, implying that the E.S. is stable. This is shown in Figure 3, where the phase trajectories are projected onto the z_1–z_2 and z_3–z_4 sub-spaces. It should be noted that since here the study is focused on the local dynamic behavior of the double pendulum system in the vicinity of a critical point, so the parameter values (μ_1, μ_2) should be chosen near the critical point $(\mu_1, \mu_2) = (0, 0)$.

If one chooses $(\mu_1, \mu_2) = (0{\cdot}03, -0{\cdot}09)$, which is located in the region where stable S.B. solutions exist, the first order approximate solution of a S.B. can be determined from the closed form expressions (22) and (18) as

$$x_1 = 0{\cdot}0588, \quad x_2 = 0{\cdot}0032, \quad x_3 = -0{\cdot}0041, \quad x_4 = 0{\cdot}0002. \tag{28}$$

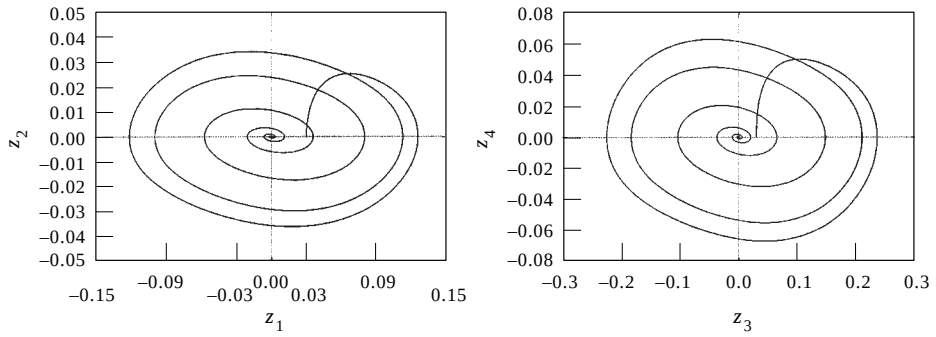

Figure 3. Trajectory starting from $(z_1, z_2, z_3, z_4) = (0{\cdot}03, 0{\cdot}0, 0{\cdot}03, 0{\cdot}0)$ converges to the E.S. when $(\mu_1, \mu_2) = (0{\cdot}18, 0{\cdot}18)$.

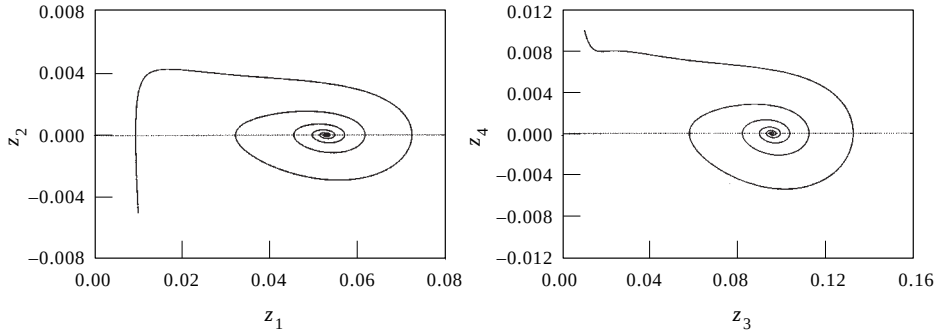

Figure 4. Trajectory starting from $(z_1, z_2, z_3, z_4) = (0{\cdot}01, -0{\cdot}01, 0{\cdot}01, 0{\cdot}01)$ converges to the S.B. when $(\mu_1, \mu_2) = (0{\cdot}03, 0{\cdot}09)$.

Then the linear transformation (15) is used to find

$$(z_1, z_2, z_3, z_4) = (0{\cdot}0625, 0{\cdot}0, 0{\cdot}1199, 0{\cdot}0). \tag{29}$$

With the parameter value $(\mu_1, \mu_2) = (0{\cdot}03, -0{\cdot}09)$, a numerical solution starting from the initial point $(z_1, z_2, z_3, z_4) = (0{\cdot}01, -0{\cdot}005, 0{\cdot}01, 0{\cdot}01)$ has been obtained, which converges to a S.B. solution $(z_1, z_2, z_3, z_4) = (0{\cdot}0526, 0{\cdot}0, 0{\cdot}0958, 0{\cdot}0)$, as shown in Figure 4. Comparing this numerical result with the approximation solution (29) indicates an error of about 20%, which is caused by the non-linearity of the system.

It is noted from equation (22) that there should be two S.B. solutions which exist simultaneously. In fact, one may see from the original system (7) that if (z_1, z_2, z_3, z_4) is a solution of equation (7), then $(-z_1, -z_2, -z_3, -z_4)$ is also a solution of the equation. Thus, when $(\mu_1, \mu_2) = (0{\cdot}03, -0{\cdot}09)$, another S.B. solution, given by $(z_1, z_2, z_3, z_4) = (-0{\cdot}0526, 0{\cdot}0, -0{\cdot}0958, 0{\cdot}0)$, is expected from the numerical computation by choosing an appropriate initial condition. Indeed, if the initial point is chosen as $(z_1, z_2, z_3, z_4) = (-0{\cdot}01, 0{\cdot}005, -0{\cdot}01, -0{\cdot}01)$, one would obtain this S.B. solution and the solution curve could be obtained by rotating the trajectory given in Figure 4 about the origin by 180°.

A stable limit cycle bifurcating from the static bifurcation solution (i.e., the 2nd H.B. solution) is obtained at the parameter value $(\mu_1, \mu_2) = (0{\cdot}0, -0{\cdot}18)$ with the initial condition $(z_1, z_2, z_3, z_4) = (0{\cdot}01, 0{\cdot}0, 0{\cdot}01, 0{\cdot}0)$, which is shown in Figure 5(a). It is noted from this figure that the trajectory starts from the right half of the z_1–z_2 and z_3–z_4 planes but finally settles down in the left half of the two planes. Further note from Figure 5(a) that, due to the symmetry of the system, one may expect that a limit cycle can also exist in the right half of the z_1–z_2 and z_3–z_4 planes if the initial condition is changed to $(z_1, z_2, z_3, z_4) = (-0{\cdot}01, 0{\cdot}0, -0{\cdot}01, 0{\cdot}0)$. This is shown in Figure 5(b). It should be noted that since the S.B. solution has both z_1 and z_3 either positive or negative, so the 2nd H.B. solutions can only have the two possibilities shown in Figure 5, and a combination of a positive (negative) z_1 and negative (positive) z_3 cannot exist. Indeed, choosing different initial conditions in the numerical computation leads only to these two periodic solutions.

To end the section, let us discuss the physical explanation of the steady state solutions obtained above. First, it can be seen from Figure 1 that the initial

equilibrium $z_i = 0$ (i.e., $\theta_1 = \theta_2 = 0$ indicating that the two rigid links are both in the vertical direction) exists for all parameter values since both P_1 and P_2 are in the vertical direction. This equilibrium solution is stable if the parameter values of (μ_1, μ_2) are chosen from the stable region bounded by the critical lines L_1 and L_2 (see Figure 2). When the parameter values are chosen from the region bounded by the critical lines L_1 and L_3, then a small perturbation will cause the initial equilibrium moving to a non-trivial stable equilibrium (S.B. solution), which is either on the left or right side of the vertical position, depending upon the perturbation. Further, when the parameters are varied so that the critical boundary L_3 is intersected, then the S.B. solution becomes unstable and a periodic vibration is initiated. The center of the vibration is located either on the left or on the right side of the vertical position, again depending on the initial perturbation.

4. A SIMPLE ZERO AND A PAIR OF PURE IMAGINARY EIGENVALUES

In order to obtain a critical point at which the system has a simple zero and a pair of pure imaginary eigenvalues, it is required that $a_4 = 0$ and $a_3(a_1 a_2 - a_3) - a_4 a_1^2 = 0$ (i.e., $a_1 a_2 = a_3$). Choosing the following parameter values:

$$f_1 = f_2 = \frac{35}{12}, \quad f_3 = \frac{35}{6}, \quad f_4 = -\frac{37}{12}, \quad f_5 = \frac{91}{12}, \quad f_6 = f_7 = 0, \quad \eta_1 = 1, \quad \eta_2 = 1, \tag{30}$$

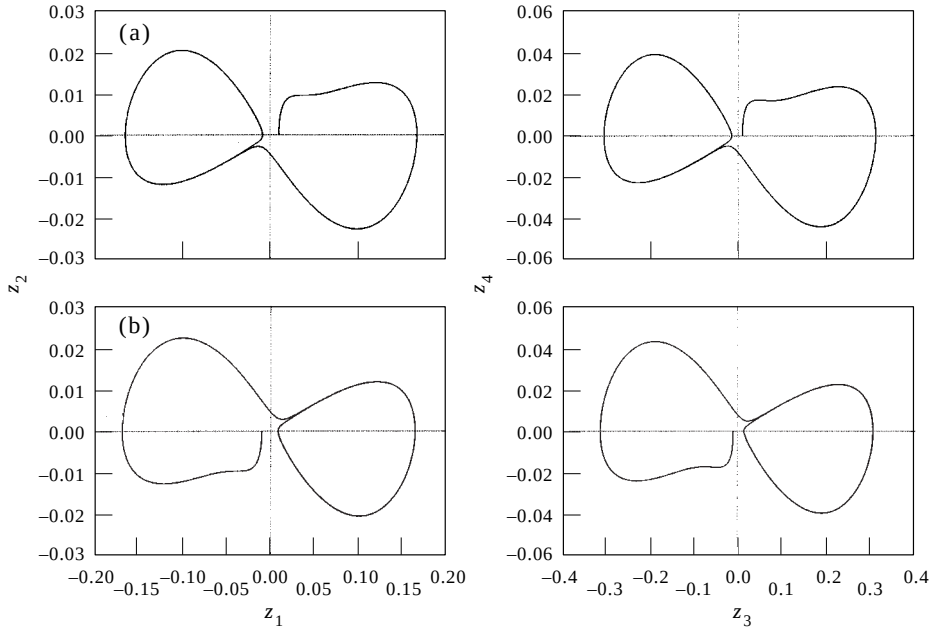

Figure 5. Trajectory converges to the 2nd H.B. for $(\mu_1, \mu_2) = (0{\cdot}0, -0{\cdot}18)$: starting from (*a*) $(z_1, z_2, z_3, z_4) = (0{\cdot}01, 0{\cdot}0, 0{\cdot}01, 0{\cdot}0)$; (b) $(z_1, z_2, z_3, z_4) = (-0{\cdot}01, 0{\cdot}0, -0{\cdot}01, 0{\cdot}0)$.

yields (see equations (10) and (11)) that $a_1 = 7/2$, $a_2 = 2/3$, $a_3 = 7/3$ and $a_4 = 0$. Thus, the Jacobian (8) has the eigenvalues:

$$\lambda_1 = 0, \quad \lambda_2 = -\frac{1}{3}\sqrt{6}I, \quad \lambda_3 = \frac{1}{3}\sqrt{6}I \quad \text{and} \quad \lambda_4 = -\frac{7}{2}. \tag{31}$$

Similar to the case of a double zero eigenvalue, one may choose f_4 and f_5 (initially, P_1 and P_2) as the parameters and use the parameter transformation

$$f_4 = -\frac{37}{12} + \mu_1, \qquad f_5 = \frac{95}{12} + \mu_2. \tag{32}$$

Then, introducing the state variable transformation

$$\begin{Bmatrix} z_1 \\ z_2 \\ z_3 \\ z_4 \end{Bmatrix} = \begin{bmatrix} 1 & 0 & 1 & 1 \\ 0 & \frac{1}{3}\sqrt{6} & 0 & -\frac{7}{2} \\ -\frac{5}{2} & -\sqrt{6} & -\frac{1}{2} & -\frac{32}{17} \\ 0 & -\frac{1}{6}\sqrt{6} & -2 & \frac{112}{17} \end{bmatrix} \begin{Bmatrix} x_1 \\ x_2 \\ x_3 \\ x_4 \end{Bmatrix} \tag{33}$$

into equation (7) yields

$$\frac{\mathrm{d}x_1}{\mathrm{d}\tau} = \left(\frac{7}{8}\mu_1 + \frac{23}{56}\mu_2\right)x_1 + \left(\frac{3}{4}\mu_1 + \frac{27}{28}\mu_2\right)x_2$$

$$+ \sqrt{6}\left(\frac{1}{2}\mu_1 - \frac{1}{14}\mu_2\right)x_3 + \left(\frac{49}{68}\mu_1 + \frac{103}{238}\mu_2\right)x_4 + Ng_1,$$

$$\frac{\mathrm{d}x_2}{\mathrm{d}\tau} = -\frac{1}{3}\sqrt{6}x_3 - \left(\frac{609}{2480}\mu_1 - \frac{297}{2480}\mu_2\right)x_1 - \left(\frac{261}{1240}\mu_1 + \frac{219}{1240}\mu_2\right)x_2$$

$$-\sqrt{6}\left(\frac{87}{620}\mu_1 - \frac{129}{620}\mu_2\right)x_3 - \left(\frac{4263}{21\,080}\mu_1 - \frac{117}{2108}\mu_2\right)x_4 + Ng_2,$$

$$\frac{\mathrm{d}x_3}{\mathrm{d}\tau} = \frac{1}{3}\sqrt{6}x_2 - \sqrt{6}\left(\frac{63}{620}\mu_1 - \frac{1}{155}\mu_2\right)x_1 - \sqrt{6}\left(\frac{14}{155}\mu_2 + \frac{27}{310}\mu_1\right)x_2$$

$$-\left(\frac{54}{155}\mu_1 - \frac{48}{155}\mu_2\right)x_3 - \sqrt{6}\left(\frac{441}{5270}\mu_1 + \frac{5}{527}\mu_2\right)x_4 + Ng_3,$$

$$\frac{dx_4}{d\tau} = -\frac{7}{2}x_4 - \left(\frac{119}{310}\mu_1 + \frac{1141}{2170}\mu_2\right)x_1 - \left(\frac{51}{155}\mu_1 + \frac{663}{1085}\mu_2\right)x_2$$

$$-\sqrt{6}\left(\frac{34}{155}\mu_1 + \frac{374}{1085}\mu_2\right)x_3 - \left(\frac{49}{155}\mu_1 + \frac{118}{217}\mu_2\right)x_4 + Ng_4, \quad (34)$$

where the non-linear functions Ng_i are given in Appendix A. Now the Jacobian matrix of equation (34) evaluated on the initial equilibrium solution $x_i = 0$ at the critical point $\mu_{1c} = \mu_{2c} = 0$ is in the Jordan canonical form

$$J_{(x_i=0)} = \begin{bmatrix} 0 & 0 & 0 & 0 \\ 0 & 0 & \frac{1}{3}\sqrt{6} & 0 \\ 0 & -\frac{1}{3}\sqrt{6} & 0 & 0 \\ 0 & 0 & 0 & -\frac{7}{2} \end{bmatrix}. \quad (35)$$

The local dynamic behaviour of the system in the vicinity of the critical point is characterized by the critical variables x_1, x_2 and x_3; and, based on equation (34), the results and formulae given in reference [4] can be applied here. Introducing a nearly identity non-linear transformation $x_i = y_i + g_i(y_j)$ (which are given by equations (B1)–(B4) in Appendix B) and a cylindrical co-ordinate transformation

$$y_1 = y, \quad y_2 = \rho\cos\theta, \quad y_3 = \rho\sin\theta, \quad y_4 = y_4, \quad (36)$$

yields the normal form of system (34) in the cylindrical co-ordinate system as follows:

$$\frac{dy}{d\tau} = y\left[\left(\frac{7}{8}\mu_1 + \frac{23}{56}\mu_2\right) - \frac{635}{1152}y^2 - \frac{1891}{192}\rho^2\right],$$

$$\frac{d\rho}{d\tau} = \rho\left[\left(-\frac{693}{2480}\mu_1 + \frac{33}{496}\mu_2\right) + \frac{175\,371}{39\,680}y^2 - \frac{230\,477}{39\,680}\rho^2\right], \quad (37)$$

and

$$\frac{d\theta}{d\tau} = \frac{1}{3}\sqrt{6}\left[1 + \frac{99}{1240}\mu_1 - \frac{111}{248}\mu_2 - \frac{222\,523}{19\,840}y^2 - \frac{373\,219}{19\,840}\rho^2\right]. \quad (38)$$

4.1. BIFURCATION ANALYSIS

The steady state solutions and their stability conditions can be found from equation (37), while equation (38) determines the frequency of possible periodic

solutions. Letting $dy/d\tau = d\rho/d\tau = 0$ in equation (37) leads to the following steady state solutions:

$$\text{E.S.:} \qquad y = \rho = 0; \tag{39}$$

$$\text{S.B.:} \qquad \begin{cases} y^2 = \dfrac{144}{4445}(49\mu_1 + 23\mu_2), \\ \rho = 0; \end{cases} \tag{40}$$

$$\text{H.B.:} \qquad \begin{cases} y = 0, \\ \rho^2 = \dfrac{528}{230\,477}(-21\mu_1 + 5\mu_2); \end{cases} \tag{41}$$

$$\left.\begin{matrix} \text{2nd H.B.} \\ \text{2nd S.B.} \end{matrix}\right\}: \qquad \begin{aligned} y^2 &= \frac{358\,125\,264}{2\,136\,112\,261}\mu_1 + \frac{553\,665\,744}{14\,952\,785\,827}\mu_2, \\ \rho^2 &= \frac{169\,733\,088}{2\,136\,112\,261}\mu_1 + \frac{84\,651\,936}{2\,136\,112\,261}\mu_2. \end{aligned} \tag{42}$$

Here, the notation "2nd H.B." denotes a dynamic bifurcation from the S.B. solution (i.e., from a non-zero equilibrium to a periodic solution), while the notation "2nd S.B." represents a static bifurcation from the H.B. solution (i.e., a periodic solution having a static shift). It should be noted that these two bifurcation solutions actually belong to the same family of limit cycles described by equation (42).

The stability conditions can be determined from the Jacobian matrix of equation (37), given by

$$J = \begin{bmatrix} \dfrac{7}{8}\mu_1 + \dfrac{23}{56}\mu_2 - \dfrac{635}{384}y^2 - \dfrac{1891}{192}\rho^2 & -\dfrac{1891}{96}y\rho \\ \dfrac{175\,371}{19\,840}y\rho & -\dfrac{693}{2480}\mu_1 + \dfrac{33}{496}\mu_2 + \dfrac{175\,371}{39\,680}y^2 - \dfrac{691\,431}{39\,680}\rho^2 \end{bmatrix}. \tag{43}$$

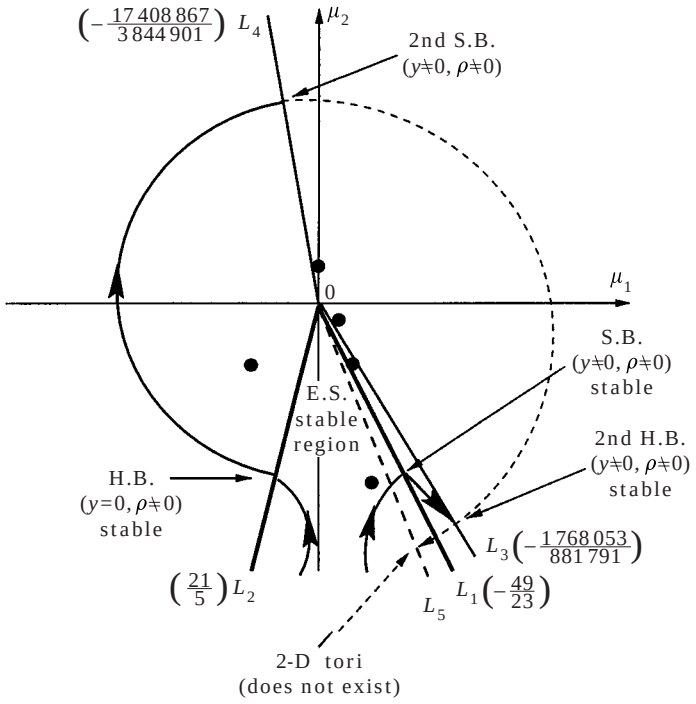

Figure 6. Bifurcation diagram for a simple zero and a pair of pure imaginary eigenvalue.

Evaluating equation (43) on the E.S. (39) shows that if the conditions

$$49\mu_1 + 23\mu_2 < 0 \quad \text{and} \quad -21\mu_1 + 5\mu_2 < 0 \tag{44}$$

are satisfied, then the E.S. is stable. The region defined by equation (44) in the parameter space is shown in Figure 6. Two critical lines which define the stability boundaries of the E.S. can be obtained from equation (44), one of them is

$$L_1: \quad 49\mu_1 + 23\mu_2 = 0 \qquad (-21\mu_1 + 5\mu_2 < 0), \tag{45}$$

from which non-trivial equilibrium solutions (S.B.) described by equation (40) bifurcate from the initial equilibrium solution (39). The other critical line is defined by

$$L_2: \quad 21\mu_1 - 5\mu_2 = 0 \qquad (49\mu_1 + 23\mu_2 < 0), \tag{46}$$

along which the H.B. solution (41) may occur.

To find the stability condition of the S.B. solution (40), evaluate the Jacobian (43) on equation (40) to obtain

$$J_{\text{S.B.}} = \begin{bmatrix} -\frac{1}{28}(49\mu_1 + 23\mu_2) & 0 \\ 0 & \frac{3}{787\,400}(1\,768\,053\mu_1 + 881\,791\mu_2) \end{bmatrix}, \tag{47}$$

which implies that the S.B. solution is stable if

$$49\mu_1 + 23\mu_2 > 0 \quad \text{and} \quad 1\,768\,053\mu_1 + 881\,791\mu_2 < 0. \tag{48}$$

The stability boundaries defined by equation (48) include the critical line L_1 (which has a slope $-2{\cdot}13$) and another critical line

$$L_3\colon 1\,768\,053\mu_1 + 881\,791\mu_2 = 0, \tag{49}$$

which has a slope $-2{\cdot}01$, larger than the slope of L_1 (i.e., the critical line L_3 is above the critical line L_1). Thus, the S.B. solution (40) is stable in the region bounded by the critical lines L_1 and L_3 (see Figure 6).

Next, the stability of the H.B. solution (41) is found by evaluating the Jacobian (43) on equation (41) to yield

$$J_{\text{H.B.}} = \begin{bmatrix} \dfrac{1}{12\,906\,712}(17\,408\,867\mu_1 + 3\,844\,901\mu_2) & 0 \\ 0 & -\dfrac{33}{1240}(-21\mu_1 + 5\mu_2) \end{bmatrix}, \tag{50}$$

which, in turn, shows when

$$17\,408\,867\mu_1 + 3\,844\,901\mu_2 < 0 \quad \text{and} \quad -21\mu_1 + 5\mu_2 > 0, \tag{51}$$

the H.B. solution is stable, and the frequency of the periodic solution (41) is given by

$$\omega_{1c} = \frac{1}{3}\sqrt{6}\left[1 - \frac{29\,477\,943}{35\,723\,935}\mu_1 - \frac{1\,658\,340}{7\,144\,787}\mu_2\right]. \tag{52}$$

The second inequality of equation (51) is satisfied since the H.B. solution appears on the left of the critical line L_2. Therefore, the region for the H.B. solution to be stable is bounded by the critical line L_2 and another critical line defined by

$$L_4\colon 17\,408\,867\mu_1 + 3\,844\,901\mu_2 = 0. \tag{53}$$

When the parameter values are varied such that the critical boundary L_3 is intersected, the S.B. solution (40) becomes unstable and bifurcates into a family of limit cycles (2nd H.B. solution). The solution of the family is given by equation (42). Similarly, the H.B. solution (41) becomes unstable on the critical boundary L_4 from which a 2nd S.B. solution occurs, leading to another family of limit cycles (42). The frequency of this family of limit cycles (2nd H.B./2nd S.B.) is given by

$$\omega_{2c} = \frac{1}{3}\sqrt{6}\left[1 - \frac{98\,798\,121}{101\,999\,092}\mu_1 - \frac{94\,213\,173}{7\,139\,930\,644}\mu_2\right]. \tag{54}$$

To investigate the stability of this family of limit cycles, evaluate the Jacobian matrix (43) on solution (42) to obtain

$$J_{\text{2nd H.B.}} = \begin{bmatrix} -\frac{635}{576}y^2 & -\frac{1891}{96}y\rho \\ \frac{175\,371}{19\,840}y\rho & -\frac{230\,477}{19\,840}\rho^2 \end{bmatrix}. \tag{55}$$

Then the stability conditions are found from the trace and determinant of the Jacobian as

$$\begin{aligned} \text{Tr} &= -\frac{635}{576}y^2 - \frac{230\,477}{19\,840}\rho^2 = -\frac{366\,816\,939\,692}{331\,097\,400\,455}\mu_1 - \frac{1\,161\,579\,452\,843}{2\,317\,681\,803\,185}\mu_2 < 0, \\ \text{Det} &= \frac{2\,136\,112\,261}{11\,427\,840}y^2\rho^2 \\ &= \frac{3}{37\,082\,908\,850\,960}(17\,68\,053\mu_1 + 881\,791\mu_2) \\ &\quad \times (17\,408\,867\mu_1 + 3\,844\,901\mu_2) > 0. \end{aligned} \tag{56}$$

It is easy to see from equations (56) that as long as the 2nd H.B. solutions exist, the two inequalities given in equations (56) are automatically satisfied. Therefore, if a 2nd H.B. solution exists, it must be stable. It is noted that letting the determinant equal zero leads to the two critical lines L_3 and L_4 which are actually the boundaries of the region where the 2nd H.B. solutions exist, and therefore stable (see Figure 6). It is also seen that letting trace equal zero results in a critical line

$$L_5\text{: } 2\,567\,718\,577\,844\mu_1 + 1\,161\,579\,452\,843\mu_2 = 0, \tag{57}$$

from which a two-dimensional torus may occur. However, it is observed that because this critical line (L_5 having slope $-2{\cdot}21$) is located below the critical line L_1 (with slope $-2{\cdot}13$), so it is not possible to have bifurcations from the 2nd H.B.

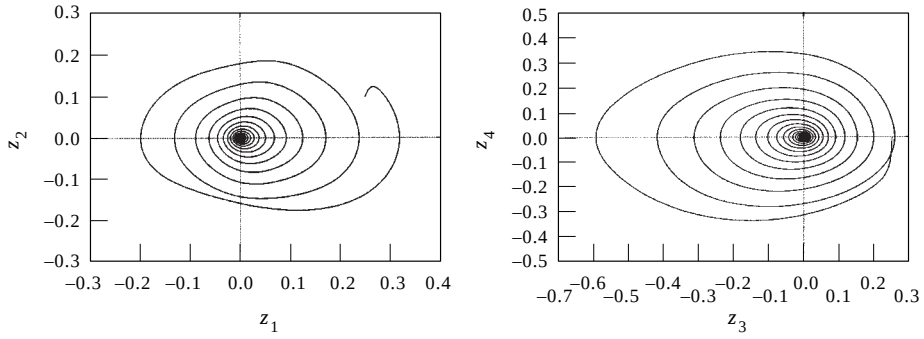

Figure 7. Trajectory starting from $(z_1, z_2, z_3, z_4) = (0{\cdot}25, 0{\cdot}1, 0{\cdot}25, 0{\cdot}0)$ converges to the E.S. when $(\mu_1, \mu_2) = (0{\cdot}1, -0{\cdot}3)$.

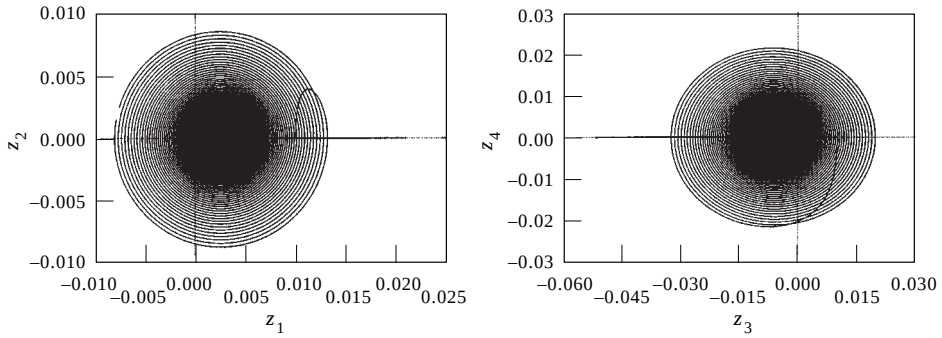

Figure 8. Trajectory starting from $(z_1, z_2, z_3, z_4) = (0{\cdot}01, 0{\cdot}0, 0{\cdot}01, 0{\cdot}0)$ converges to the S.B. when $(\mu_1, \mu_2) = (0{\cdot}01, -0{\cdot}0205)$.

solutions, leading to two-dimensional tori. The critical bifurcation lines are illustrated in Figure 6.

4.2. NUMERICAL RESULTS

Similar to the case of a double zero eigenvalue, different parameter values are chosen from the different regions shown by the black circle dots in Figure 6 to confirm the analytical results obtained in the previous subsection. When the parameter values are chosen as $(\mu_1, \mu_2) = (0{\cdot}1, -0{\cdot}3)$, which is located in the region bounded by the critical lines L_1 and L_2, numerical results show that a trajectory starting from a point near the origin converges to the origin asymptotically. An example is shown in Figure 7, in which the initial condition is $(z_1, z_2, z_3, z_4) = (0{\cdot}25, 0{\cdot}1, 0{\cdot}25, 0{\cdot}0)$.

Since the region for the existence of a stable S.B. solution is very small, located between the two critical lines L_1 (with slope $-2{\cdot}13$) and L_3 (having slope $-2{\cdot}01$), it is very difficult to find suitable parameter values leading to a S.B. solution without an analytic study. Figure 8 shows an example of stable S.B. solutions when $(\mu_1, \mu_2) = (0{\cdot}01, -0{\cdot}0205)$. The initial starting point of the trajectory is $(z_1, z_2, z_3, z_4) = (0{\cdot}01, 0{\cdot}0, 0{\cdot}01, 0{\cdot}0)$. It is interesting to note that the trajectory first converges to the dark area and then moves along the z_2-axis and z_4-axis to the non-zero equilibrium. The numerical S.B. solution for this case is $(z_1, z_2, z_3, z_4) = (0{\cdot}0211, 0{\cdot}0, -0{\cdot}0519, 0{\cdot}0)$. It should be noted that due to symmetry of the system another S.B. solution, given by $(z_1, z_2, z_3, z_4) = (-0{\cdot}0211, 0{\cdot}0, 0{\cdot}0519, 0{\cdot}0)$, can be obtained numerically if the initial condition is chosen, say, as $(z_1, z_2, z_3, z_4) = (-0{\cdot}01, 0{\cdot}0, -0{\cdot}01, 0{\cdot}0)$.

The analytic S.B. solution for $(\mu_1, \mu_2) = (0{\cdot}1, -0{\cdot}3)$ can be obtained through equations (36) and (40) and the non-linear transformations (B1)–(B4) as

$$x_1 = 0{\cdot}02448, \qquad x_2 = -0{\cdot}0002, \qquad x_3 = -0{\cdot}0001, \qquad x_4 = 0{\cdot}0001. \quad (58)$$

Then use the linear transformation (33) to find

$$z_1 = 0{\cdot}0243, \qquad z_2 = -0{\cdot}0003, \qquad z_3 = -0{\cdot}0612, \qquad z_4 = 0{\cdot}0003, \quad (59)$$

which is close to the numerical result, showing that even the first order approximate perturbation solution gives a good prediction.

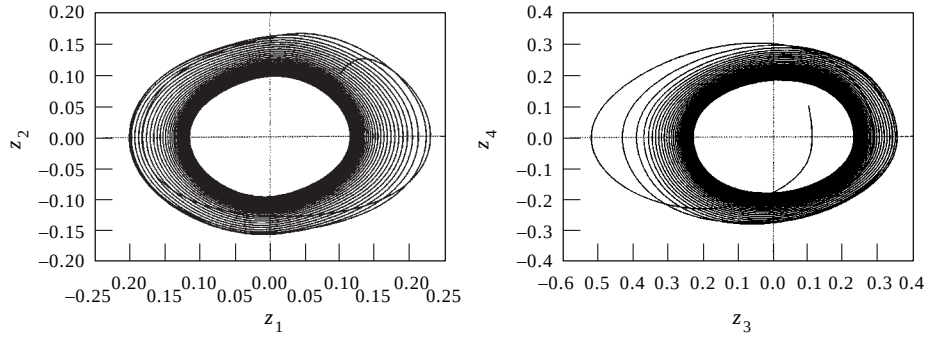

Figure 9. Trajectory starting from $(z_1, z_2, z_3, z_4) = (0{\cdot}1, 0{\cdot}1, 0{\cdot}1, 0{\cdot}1)$ converges to the H.B. when $(\mu_1, \mu_2) = (-0{\cdot}1, -0{\cdot}1)$.

Next, choosing $(\mu_1, \mu_2) = (-0{\cdot}1, -0{\cdot}1)$ yields a stable limit cycle shown in Figure 9. The periodic trajectory of the H.B. solution starts from the initial point $(z_1, z_2, z_3, z_4) = (0{\cdot}1, 0{\cdot}1, 0{\cdot}1, 0{\cdot}1)$, and the amplitude of the limit cycles is about 0·1 for z_1–z_2 variables and 0·2 for z_3–z_4 variables. With the aid of the formulae (33), (36), (41) and the non-linear transformations (B1)–(B4), one may find the estimation of the approximate periodic solution at $t = 0$ (remember that the system is autonomous) as

$$z_1 = -0{\cdot}0117, \qquad z_2 = -0{\cdot}0171, \qquad z_3 = -0{\cdot}1073, \qquad z_4 = 0{\cdot}0342. \quad (60)$$

Thus, $\sqrt{z_1^2 + z_2^2} = 0{\cdot}0207$ and $\sqrt{z_3^2 + z_4^2} = 0{\cdot}1126$, which is not in a good agreement with the numerical results, but still gives a good qualitative prediction.

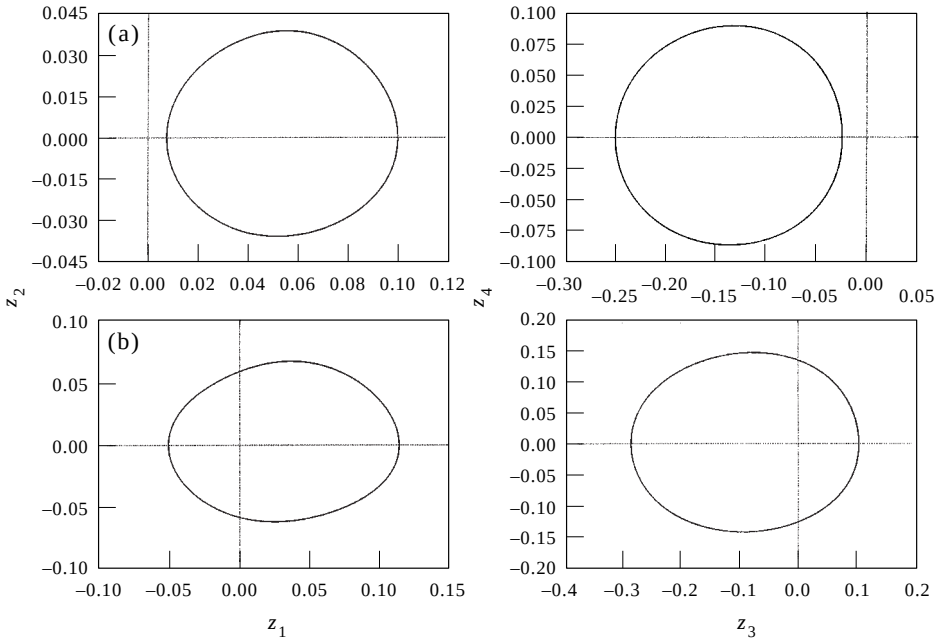

Figure 10. 2nd H.B. solutions for: (a) $(\mu_1, \mu_2) = (0{\cdot}02, -0{\cdot}03)$; (b) $(\mu_1, \mu_2) = (0{\cdot}0, 0{\cdot}05)$.

Two numerical secondary bifurcation solutions (2nd H.B. and 2nd S.B. solutions) are obtained by choosing $(\mu_1, \mu_2) = (0{\cdot}02, -0{\cdot}03)$ with the initial condition $(z_1, z_2, z_3, z_4) = (0{\cdot}15, 0{\cdot}04, 0{\cdot}25, 0{\cdot}08)$ and $(\mu_1, \mu_2) = (0{\cdot}00, 0{\cdot}05)$ with the initial condition $(z_1, z_2, z_3, z_4) = (0{\cdot}1, 0{\cdot}05, 0{\cdot}1, 0{\cdot}07)$; the former is close to the critical line L_3 while the latter is near the critical line L_4. These 2nd H.B./2nd S.B. solutions are depicted in Figure 10. It should be noted that the center of the H.B. solution (see Figure 9) is located at the origin, indicating that the limit cycle bifurcates from the initial equilibrium. However, the center of the periodic solutions shown in Figure 10 is located at a non-zero position, implying that it is either a 2nd H.B. solution bifurcating from the S.B. solution (40) or a 2nd S.B. solution bifurcating from the H.B. solution (41). The solution of this family of limit cycles is given by equation (42) in which y can take both positive and negative signs, again implying that another 2nd H.B. solution exists for the same parameter values and is symmetric to the one given in Figure 10 about the origin. It should be noted from Figure 10 that the transient part of the trajectory has been omitted for a clear view of the steady state solutions.

Again from the analytic results, one may find the following estimations for the 2nd H.B./2nd S.B. solutions:

$$\begin{aligned} z_1 &= 0{\cdot}0463, \quad z_2 = 0{\cdot}0151 \quad \text{when } z_2 \text{ reaches its maximum,} \\ z_3 &= -0{\cdot}1262, \quad z_4 = -0{\cdot}0468 \quad \text{when } z_4 \text{ reaches its maximum,} \end{aligned} \tag{61}$$

for $(\mu_1, \mu_2) = (0{\cdot}02, -0{\cdot}03)$; and

$$\begin{aligned} z_1 &= 0{\cdot}0306, \quad z_2 = 0{\cdot}0253 \quad \text{when } z_2 \text{ reaches its maximum,} \\ z_3 &= -0{\cdot}0892, \quad z_4 = -0{\cdot}1221 \quad \text{when } z_4 \text{ reaches its maximum,} \end{aligned} \tag{62}$$

for $(\mu_1, \mu_2) = (0{\cdot}00, 0{\cdot}05)$. These results show a prediction close to the numerical results.

The physical explanation of this case is similar to the case of a double zero eigenvalue studied in the previous section. However, here it indicates a possibility of existence of a Hopf bifurcation, which gives a vibration with its center located on the vertical line $\theta_1 = \theta_2 = 0$ (i.e., $z_i = 0$).

5. TWO PAIRS OF PURE IMAGINARY EIGENVALUES

In this case, it is required that $a_1 = a_3 = 0$ at a critical point. If the values of the parameters defined in equation (6) are chosen as

$$f_1 = \frac{4}{7}, \quad f_2 = \frac{407}{56}, \quad f_5 = \frac{1}{56}, \quad f_4 = \frac{535}{28}, \quad f_5 = f_6 = 0, \quad f_7 = -1, \quad \eta_1 = \eta_2 = 0, \tag{63}$$

then, it is easy to find from equations (10) and (11) that $a_1 = a_3 = 0$, $a_2 = 3$ and $a_4 = 2$, which indicates that the Jacobian (8) has two pairs of pure imaginary eigenvalues:

$$\lambda_{1,2} = \pm I \quad \text{and} \quad \lambda_{3,4} = \pm\sqrt{2}I \ (I^2 = -1). \tag{64}$$

Now, choosing η_1 and η_2 (initially, d_1 and d_2) as the parameters, using the parameter transformation

$$\eta_1 = \mu_1, \qquad \eta_2 = \mu_2, \tag{65}$$

and then introducing the state variable transformation

$$\begin{Bmatrix} z_1 \\ z_2 \\ z_3 \\ z_4 \end{Bmatrix} = \begin{bmatrix} \frac{16}{21} & 0 & \frac{2}{7}\sqrt{2} & 0 \\ 0 & \frac{16}{21} & 0 & \frac{4}{7} \\ 1 & 0 & \frac{1}{2}\sqrt{2} & 0 \\ 0 & 1 & 0 & 1 \end{bmatrix} \begin{Bmatrix} x_1 \\ x_2 \\ x_3 \\ x_4 \end{Bmatrix} \tag{66}$$

into equation (7) yields

$$\frac{\mathrm{d}x_1}{\mathrm{d}\tau} = x_2,$$

$$\frac{\mathrm{d}x_2}{\mathrm{d}\tau} = -x_1 - \left(\frac{22}{7}\mu_1 - \frac{75}{28}\mu_2\right)x_2 - \left(\frac{33}{14}\mu_1 - \frac{135}{28}\mu_2\right)x_4 + Nh_1,$$

$$\frac{\mathrm{d}x_3}{\mathrm{d}\tau} = \sqrt{2}x_4,$$

$$\frac{\mathrm{d}x_4}{\mathrm{d}\tau} = -\sqrt{2}x_3 + \left(\frac{74}{21}\mu_1 - \frac{265}{84}\mu_2\right)x_2 + \left(\frac{37}{14}\mu_1 - \frac{159}{28}\mu_2\right)x_4 + Nh_2, \tag{67}$$

where the non-linear functions Nh_i are listed in Appendix A. With the aid of normal form theory, similarly one may use a non-linear transformation $x_i = y_i + g_i(y_j)$ (given by equations (B5)–(B8) in Appendix B) and introduce a transformation

$$y_1 = \rho_1 \cos\theta_1, \qquad y_2 = \rho_1 \sin\theta_1, \qquad y_3 = \rho_2 \cos\theta_2, \qquad y_4 = \rho_2 \sin\theta_2, \tag{68}$$

to obtain the normal form in a polar co-ordinate system:

$$\frac{\mathrm{d}\rho_1}{\mathrm{d}\tau} = \rho_1\left[-\frac{11}{7}\mu_1 + \frac{75}{56}\mu_2 - \frac{625}{10\,976}\rho_1^2 - \frac{2025}{5488}\rho_2^2\right],$$

$$\frac{\mathrm{d}\rho_2}{\mathrm{d}\tau} = \rho_2\left[-\frac{37}{28}\mu_1 - \frac{159}{56}\mu_2 + \frac{1325}{5488}\rho_1^2 + \frac{4293}{10\,976}\rho_2^2\right]; \tag{69}$$

and

$$\frac{d\theta_1}{d\tau} = 1 - \frac{6\,493\,901}{22\,127\,616}\rho_1^2 - \frac{1\,423\,069}{2\,458\,624}\rho_2^2,$$

$$\frac{d\theta_2}{d\tau} = \sqrt{2}\left[1 + \frac{14\,046\,397}{22\,127\,616}\rho_1^2 + \frac{2\,975\,501}{9\,834\,496}\rho_2^2\right]. \tag{70}$$

5.1. BIFURCATION ANALYSIS

On the basis of equation (69), the steady state solutions are obtained by setting $d\rho_1/d\tau = d\rho_2/d\tau = 0$ as follows:

(1) The initial equilibrium solution (E.S.):

$$\rho_1 = \rho_2 = 0 \qquad (\text{i.e., } x_i = 0). \tag{71}$$

(2) Hopf bifurcation solution (H.B.(I) with frequency ω_1):

$$\rho_1^2 = \frac{10\,976}{625}\left(-\frac{11}{7}\mu_1 + \frac{75}{56}\mu_2\right), \qquad \rho_2 = 0,$$

$$\omega_1 = 1 + \frac{71\,432\,911}{8\,820\,000}\mu_1 - \frac{6\,493\,901}{940\,800}\mu_2. \tag{72}$$

(3) Hopf bifurcation solution (H.B.(II) with frequency ω_2):

$$\rho_1 = 0, \qquad \rho_2^2 = -\frac{10\,976}{4293}\left(\frac{37}{28}\mu_1 - \frac{159}{56}\mu_2\right),$$

$$\omega_2 = \sqrt{2}\left[1 - \frac{110\,093\,537}{107\,702\,784}\mu_1 + \frac{2\,975\,501}{1\,354\,752}\mu_2\right]. \tag{73}$$

(4) Quasi-periodic solution (2-D tori with frequencies ω_1, ω_2):

$$\rho_1^2 = \frac{188\,944}{99\,375}\mu_1 + \frac{196}{25}\mu_2, \qquad \rho_2^2 = -\frac{1\,465\,688}{321\,975}\mu_1 + \frac{196}{81}\mu_2.$$

$$\omega_1 = 1 + \frac{104\,850\,832\,237}{50\,485\,680\,000}\mu_1 - \frac{47\,010\,917}{12\,700\,800}\mu_2,$$

$$\omega_2 = \sqrt{2}\left[1 - \frac{34\,401\,875\,231}{201\,942\,720\,000}\mu_1 + \frac{580\,057\,817}{101\,606\,400}\mu_2\right]. \tag{74}$$

The Jacobian matrix of equation (69) takes the form

$$J = \begin{bmatrix} -\frac{11}{7}\mu_1 + \frac{75}{56}\mu_2 - \frac{1875}{10\,976}\rho_1^2 - \frac{2025}{5488}\rho_2^2 & -\frac{2025}{2744}\rho_1\rho_2 \\ \frac{1325}{2744}\rho_1\rho_2 & \frac{37}{28}\mu_1 - \frac{159}{56}\mu_2 + \frac{1325}{5488}\rho_1^2 + \frac{12\,879}{10\,976}\rho_2^2 \end{bmatrix}, \quad (75)$$

which can be used for the stability analysis of the above steady state solutions. Evaluating the Jacobian (75) on the fundamental equilibrium solution (71) results in the stable region for the E.S. as

$$-\frac{11}{7}\mu_1 + \frac{75}{56}\mu_2 < 0 \quad \text{and} \quad \frac{37}{28}\mu_1 - \frac{159}{56}\mu_2 < 0, \quad (76)$$

which, in turn, gives two critical lines. One of these is described by

$$L_1: 88\mu_1 - 75\mu_2 = 0 \qquad (74\mu_1 - 159\mu_2 < 0), \quad (77)$$

which leads to a family of limit cycles bifurcating from the E.S. with the approximate solution H.B.(I) given in equation (72). The second critical line is

$$L_2: 74\mu_1 - 159\mu_2 = 0 \qquad (88\mu_1 - 75\mu_2 > 0), \quad (78)$$

from which another family of limit cycles, given by H.B.(II) solution (73), may occur.

Next, evaluating the Jacobian matrix (75) on the Hopf bifurcation solution (72) results in the stability conditions

$$-7478\mu_1 + 3975\mu_2 < 0 \qquad (88\mu_1 - 75\mu_2 < 0) \quad (79)$$

for the H.B.(I) solution. The inequality given in equation (79) implies another critical line

$$L_3: \quad 7478\mu_1 - 3975\mu_2 = 0 \qquad (74\mu_1 - 159\mu_2 > 0), \quad (80)$$

along which a secondary Hopf bifurcation with frequency ω_2 takes place from the first bifurcating limit cycle H.B.(I), leading to a 2-D torus described by solution (74).

Similarly, a set of stability conditions associated with the H.B.(II) solution (73) can be obtained by evaluating the Jacobian (75) of this solution. Thus, for the H.B.(II) solution to be stable, the inequalities

$$-964\mu_1 - 3975\mu_2 < 0 \quad \text{and} \quad 74\mu_1 - 159\mu_2 > 0 \quad (81)$$

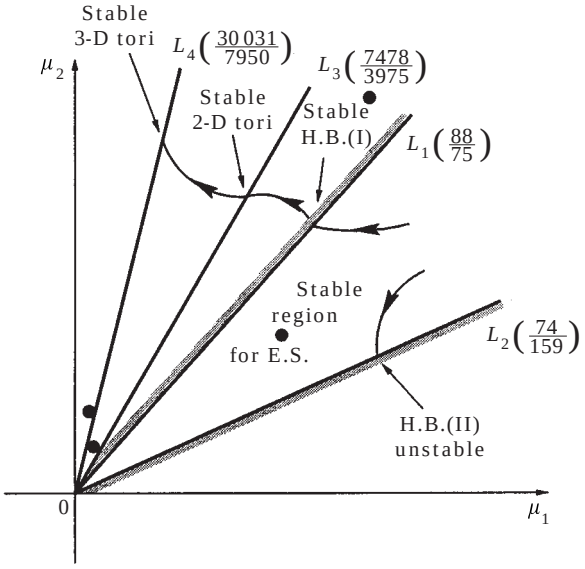

Figure 11. Bifurcation diagram for two pairs of pure imaginary eigenvalue.

must be satisfied. The first inequality in equation (81) is always satisfied if μ_1 and μ_2 are positive (positive damping as assumed). However, it can be seen from equation (73) that the existence of the H.B.(II) solution requires $74\mu_1 - 159\mu_2 < 0$ which violates the second stability condition given in equation (81). Thus, the H.B.(II) solution (73) is unstable.

To find the stability of the family of 2-D tori expressed by equation (74), evaluating the Jacobian (75) on equation (74) yields

$$J_{2-\text{D tori}} = \begin{bmatrix} -\frac{625}{5488}\rho_1^2 & -\frac{2025}{2744}\rho_1\rho_2 \\ \frac{1325}{2744}\rho_1\rho_2 & \frac{4293}{5488}\rho_2^2 \end{bmatrix} . \tag{82}$$

The stability conditions are then obtained from the trace and determinant of the Jacobian as

$$\text{Tr} = -\frac{625}{5488}\rho_1^2 + \frac{4293}{5488}\rho_2^2 = -\frac{30\,031}{7950}\mu_1 + \mu_2 < 0,$$

$$\text{Det} = \frac{8\,006\,445}{30\,118\,144}\rho_1^2\rho_2^2 = -\frac{1}{3\,116\,400}(964\mu_1 + 3975\mu_2)(7478\mu_1 - 3975\mu_2) > 0. \tag{83}$$

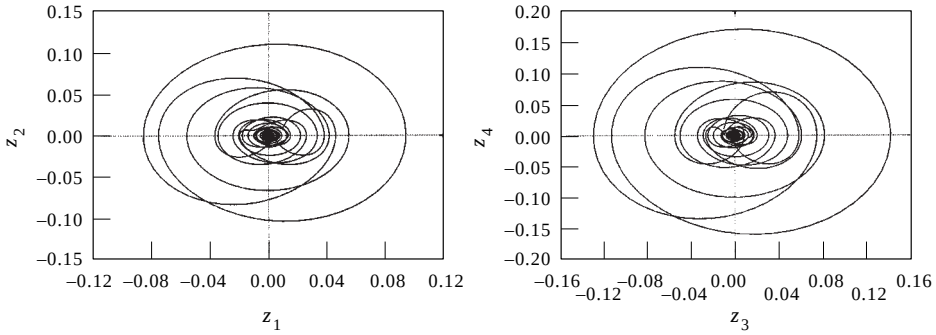

Figure 12. Trajectory starting from $(z_1, z_2, z_3, z_4) = (0{\cdot}01, 0{\cdot}01, -0{\cdot}01, 0{\cdot}01)$ converges to the E.S. when $(\mu_1, \mu_2) = (0{\cdot}05, 0{\cdot}04)$.

It is easy to see that the second inequality in equation (83) is automatically satisfied as long as a solution (ρ_1, ρ_2) exists for a motion on the 2-D torus. In fact, the existence of a 2-D torus, found from equation (74), requires $7478\mu_1 - 3975\mu_2 < 0$, which implies the critical boundary L_3. The first inequality in equation (83), on the other hand, leads to a critical line:

$$L_4: \quad 30\,031\mu_1 - 7950\mu_2 = 0, \tag{84}$$

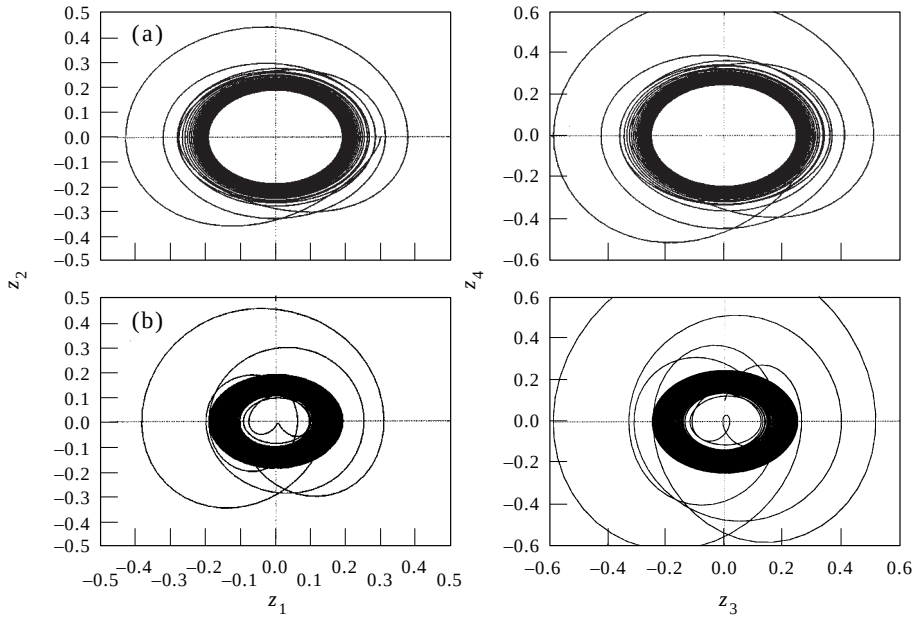

Figure 13. H.B. solutions for $(\mu_1, \mu_2) = (0{\cdot}05, 0{\cdot}095)$: starting from (a) $(z_1, z_2, z_3, z_4) = (0{\cdot}3, 0{\cdot}0, 0{\cdot}3, 0{\cdot}0)$; (b) $(z_1, z_2, z_3, z_4) = (0{\cdot}1, 0{\cdot}0, 0{\cdot}0, 0{\cdot}1)$.

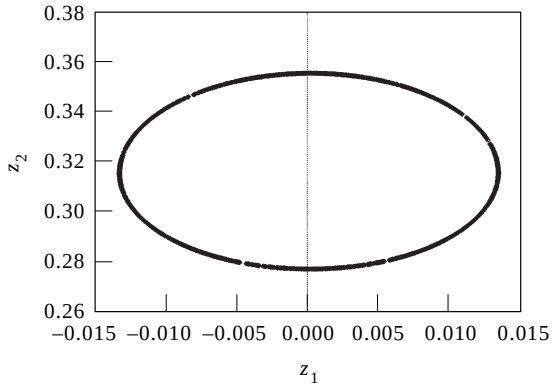

Figure 14. The Poincare map of a 2-D torus projected onto the plane $z_3 = 0$, $z_2 \geqslant 0$ for $(\mu_1, \mu_2) = (0{\cdot}005, 0{\cdot}015)$.

from which a quasi-periodic solution (2-D torus) loses stability and bifurcates into a motion on a 3-D torus $(\omega_1, \omega_2, \omega_3)$; the third frequency of the 3-D torus, ω_3, is given by

$$\omega_3 = \sqrt{\frac{8\,049\,375}{15\,059\,072}}\,\rho_1\rho_2 = \frac{1}{\sqrt{3\,116\,400}}\sqrt{(964\mu_1 + 3975\mu_2)(3975\mu_2 - 7478\mu_1)}. \tag{85}$$

The critical bifurcation lines are illustrated in Figure 11.

5.2. NUMERICAL RESULTS

By choosing a point in the parameter space as $(\mu_1, \mu_2) = (0{\cdot}05, 0{\cdot}04)$, which is located in the stable region for the E.S., one can find a numerical solution, as shown in Figure 12. The trajectory starting from the initial point $(z_1, z_2, z_3, z_4) = (0{\cdot}01, 0{\cdot}01, -0{\cdot}01, 0{\cdot}01)$ converges to the origin—the E.S. of the system.

When $(\mu_1, \mu_2) = (0{\cdot}075, 0{\cdot}095)$, a Hopf bifurcation solution H.B.(I) is obtained, as shown in Figure 13, where two initial points are chosen as $(z_1, z_2, z_3, z_4) = (0{\cdot}3, 0{\cdot}0, 0{\cdot}3, 0{\cdot}0)$ and $(z_1, z_2, z_3, z_4) = (0{\cdot}1, 0{\cdot}0, 0{\cdot}0, 0{\cdot}1)$. Both trajectories converge to a limit cycle, one from the outside of the limit cycle, the other from inside the limit cycle. From equation (72) one can find the amplitude of the periodic solution as $\rho_1 = 0{\cdot}9244$ with frequency $\omega_1 = 0{\cdot}7492$. Thus, the first order approximation of the H.B.(I) solution may be obtained using the general non-linear transformation given in reference [5] as

$$\begin{aligned}
x_1 &= 0{\cdot}9244\cos(0{\cdot}7429\tau) + 0{\cdot}0454\cos 3(0{\cdot}7429\tau) + 0{\cdot}0037\sin 3(0{\cdot}7429\tau),\\
x_2 &= -0{\cdot}6923\sin(0{\cdot}7429\tau) + 0{\cdot}0112\cos 3(0{\cdot}7429\tau) - 0{\cdot}1353\sin 3(0{\cdot}7429\tau),\\
x_3 &= -0{\cdot}5378\sqrt{2}\cos(0{\cdot}7429\tau) + 0{\cdot}0084\sqrt{2}\sin(0{\cdot}7429\tau)\\
&\quad - 0{\cdot}0607\sqrt{2}\cos 3(0{\cdot}7429\tau) - 0{\cdot}0050\sqrt{2}\sin 3(0{\cdot}7429\tau),\\
x_4 &= 0{\cdot}0084\cos(0{\cdot}7429\tau) + 0{\cdot}5378\sin(0{\cdot}7429\tau)\\
&\quad - 0{\cdot}0151\cos 3(0{\cdot}7429\tau) + 0{\cdot}1820\sin 3(0{\cdot}7429\tau).
\end{aligned} \tag{86}$$

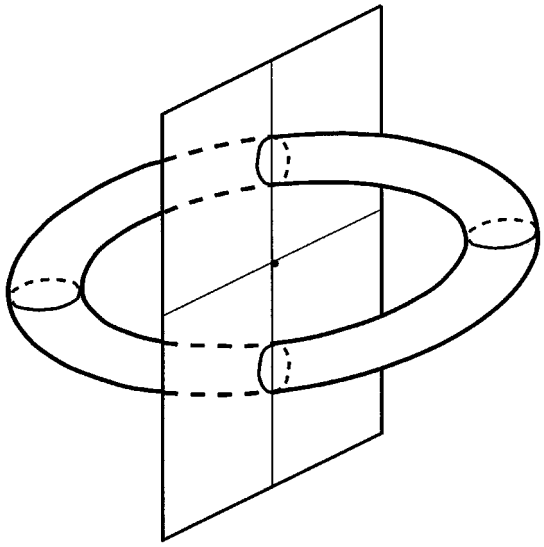

Figure 15. A two-dimensional torus in the four-dimensional state space.

To estimate the amplitude of the periodic solution from equation (86) in terms of the original variables z_i's, letting $t = 0$ and using the transformation (66) yields the first order approximate solution for z_i:

$$z_1 = 0{\cdot}3969, \qquad z_2 = 0{\cdot}0047, \qquad z_3 = 0{\cdot}3713, \qquad z_4 = 0{\cdot}0045. \tag{87}$$

This shows that the amplitude of the approximate periodic solution obtained from the analytic formula is about 0·4, which is almost twice that of the numerical results. This large error suggests that high order approximations are needed to achieve a more accurate approximate prediction.

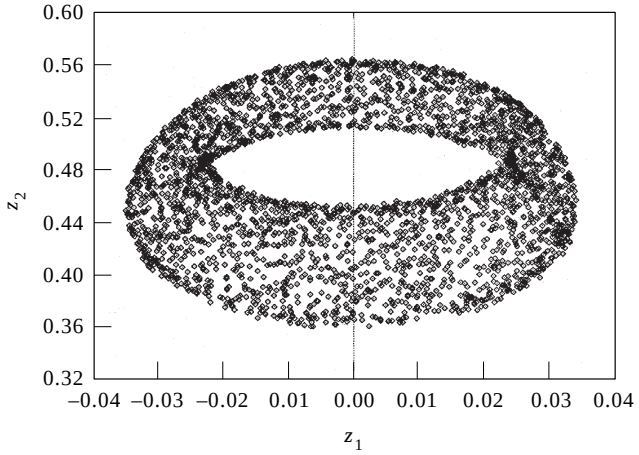

Figure 16. The Poincare map of a 3-D torus projected onto the plane $z_3 = 0$, $z_2 \geqslant 0$ for $(\mu_1, \mu_2) = (0{\cdot}005, 0{\cdot}03)$.

A numerical solution for a quasi-periodic motion on a 2-D torus is obtained by choosing the parameter values as $(\mu_1, \mu_2) = (0{\cdot}005, 0{\cdot}015)$, which is located in the region bounded by the critical lines L_1 and L_3. In order to show this 2-D torus, the trajectory z_i in the four-dimensional state space is projected onto the half plane $z_3 = 0$, $z_2 \geqslant 0$ to obtain a Poincare map, as shown in Figure 14. Since the Poincare map is a dense periodic orbit, so the solution is indeed a quasi-periodic motion on a 2-D torus. It should be noted that due to symmetry of the system, another Poincare map exists, which is symmetric to the one shown in Figure 14 about the z_1-axis, on the half plane $z_3 = 0$, $z_2 \leqslant 0$. One may image that the 2-D torus passes the two ellipses (see Figure 15).

The two amplitudes of the quasi-periodic motions corresponding to the parameter values $(\mu_1, \mu_2) = (0{\cdot}005, 0{\cdot}015)$ can be estimated from equation (74) as $\rho_1 = 0{\cdot}3565$, $\rho_2 = 0{\cdot}1164$. Similar to the above Hopf bifurcation solution, one may let $t = 0$, and use the non-linear transformation [5] to obtain the approximate solution

$$x_1 = 0{\cdot}3442, \qquad x_2 = 0{\cdot}0034, \qquad x_3 = 0{\cdot}0543, \qquad x_4 = -0{\cdot}0010. \tag{88}$$

Then applying the linear transformation (66) yields

$$z_1 = 0{\cdot}2842, \qquad z_2 = 0{\cdot}0021, \qquad z_3 = 0{\cdot}3826, \qquad z_4 = 0{\cdot}0025 \tag{89}$$

which gives $\sqrt{z_1^2 + z_2^2} = 0{\cdot}2842$ and $\sqrt{z_3^2 + z_4^2} = 0{\cdot}3826$. The amplitudes of the quasi-periodic motion found from the numerical results are $\sqrt{z_1^2 + z_2^2} = 0{\cdot}3571$ and $\sqrt{z_3^2 + z_4^2} = 0{\cdot}3675$. This shows that the first order analytic approximate solution gives a reasonable prediction, at least from the viewpoint of qualitative behaviour.

Finally, if the parameter values are chosen as $(\mu_1, \mu_2) = (0{\cdot}005, 0{\cdot}03)$, which is located in the region bounded by the critical line L_4 and the positive μ_2-axis, where quasi-periodic motions on a 3-D torus may arise, as indicated by the analytic study given in the previous subsection. The numerical result is shown in Figure 16, which is again a projection of the trajectory onto the half plane $z_3 = 0$, $z_2 \geqslant 0$. It can be seen from this figure that the Poincare map now shows a dense 2-D torus, implying that the quasi-periodic motion is indeed on a 3-D torus embedded in the four-dimensional state space.

The quasi-periodic motion on a 2-D torus can be imaged as a combined motion via the superposition of a small periodic motion (ω_2) on the main periodic vibration (ω_1) which has its center at the origin $z_i = 0$. Then the quasi-periodic motion on a 3-D torus can be viewed as a motion by adding a third small periodic motion (ω_3) to the 2-D quasi-periodic motion. It is expected that these complex motions may be observed from a real experiment in a laboratory.

6. 1:1 RESONANCE

The non-resonant case for the two pairs of pure imaginary eigenvalues has been studied in detail in the previous section; we now turn to the primary 1:1 resonant case. Suppose that the Jacobian (8) has two repeated pairs of pure imaginary

eigenvalues $\lambda_{1,2} = \lambda_{3,4} = \pm i$. This means that $a_1 = a_3 = 0$, $a_2 = 2$ and $a_4 = 1$. One choice of the parameter values satisfying these conditions is

$$f_1 = 10, \quad f_2 = 2, \quad f_3 = 5, \quad f_4 = -6, \quad f_5 = 8, \quad f_6 = -10,$$
$$f_7 = 30, \quad \eta_1 = \eta_2 = 0. \tag{90}$$

Again choosing η_1 and η_2 as the parameters, and then using the parameter transformation $\eta_1 = \mu_1$, $\eta_2 = \mu_2$, and the state variable transformation

$$\begin{Bmatrix} z_1 \\ z_2 \\ z_3 \\ z_4 \end{Bmatrix} = \begin{bmatrix} 0 & 1 & 0 & 0 \\ -1 & 0 & 0 & 1 \\ 0 & 1 & -2 & 0 \\ -1 & 0 & 0 & -1 \end{bmatrix} \begin{Bmatrix} x_1 \\ x_2 \\ x_3 \\ x_4 \end{Bmatrix} \tag{91}$$

yields the system

$$\frac{\mathrm{d}x_1}{\mathrm{d}\tau} = x_2 + x_3 - \mu_2 x_4 - \frac{8}{3}x_2^3 + 10x_3^3 - 120x_4^3$$
$$- x_1^2 x_3 + 11x_2^2 x_3 - 16x_2 x_3^2 - x_3 x_4^2 + 2x_1 x_3 x_4,$$
$$\frac{\mathrm{d}x_2}{\mathrm{d}\tau} = -x_1 + x_4, \qquad \frac{\mathrm{d}x_3}{\mathrm{d}\tau} = x_4,$$
$$\frac{\mathrm{d}x_4}{\mathrm{d}\tau} = -x_3 + \frac{1}{2}\mu_1 x_1 - \frac{1}{2}\mu_1 x_4 - 3\mu_2 x_4 - 5x_1^3 - \frac{10}{3}x_2^3 + \frac{62}{3}x_3^3 - 355x_4^3$$
$$- 3x_1^2 x_3 + 15x_1^2 x_4 + 17x_2^2 x_3 - 28x_2 x_3^2 - 15x_1 x_4^2 - 3x_3 x_4^2 + 2x_1 x_3 x_4, \tag{92}$$

with the Jacobian matrix evaluated at the critical point $\mu_1 = \mu_2 = 0$ in the Jordan canonical form

$$J = \begin{bmatrix} 0 & 1 & 1 & 0 \\ -1 & 0 & 0 & 1 \\ 0 & 0 & 0 & 1 \\ 0 & 0 & -1 & 0 \end{bmatrix}, \tag{93}$$

which is a so called non-semisimple form. By using a non-linear transformation $x_i = y_i + g_i(y_j)$, which is given by equations (B9)–(B12) in Appendix B, and the

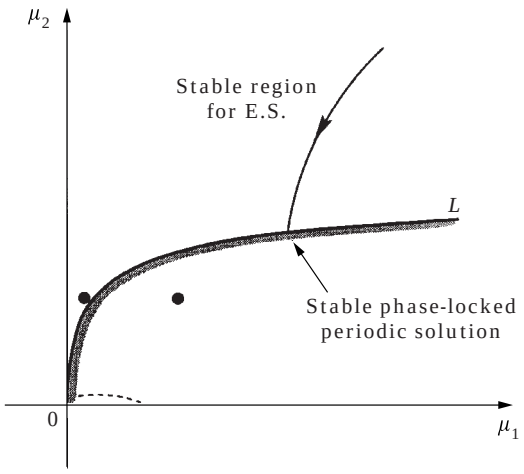

Figure 17. Bifurcation diagram for the 1:1 resonant case.

transformation (67), one may find the normal form as follows:

$$\frac{d\rho_1}{d\tau} = \rho_2 \cos(\theta_2 - \theta_1),$$

$$\begin{aligned}\frac{d\rho_2}{d\tau} = &-\frac{1}{4}\mu_1\rho_2 - \frac{3}{2}\mu_2\rho_2 - \frac{1}{4}\mu_1\rho_1 \sin(\theta_2 - \theta_1) + 15\rho_1^2\rho_2 + 30\rho_1\rho_2^2 \sin(\theta_2 - \theta_1) \\ &- 80\rho_1\rho_2^2 \cos(\theta_2 - \theta_1) + \frac{15}{2}\rho_1^3 \sin(\theta_2 - \theta_1) - 5\rho_1^3 \cos(\theta_2 - \theta_1) \\ &+ 6\rho_1^2\rho_2 \sin 2(\theta_2 - \theta_1) - \frac{15}{2}\rho_1^2\rho_2 \cos 2(\theta_2 - \theta_1),\end{aligned}$$

$$\rho_1 \frac{d\theta_1}{d\tau} = \rho_1 + \rho_2 \sin(\theta_2 - \theta_1),$$

$$\begin{aligned}\rho_2 \frac{d\theta_2}{d\tau} = \rho_2 &- \frac{1}{4}\mu_1\rho_1 \cos(\theta_2 - \theta_1) - 22\rho_1^2\rho_2 + 80\rho_1\rho_2^2 \sin(\theta_2 - \theta_1) \\ &+ 30\rho_1\rho_2^2 \cos(\theta_2 - \theta_1) \\ &+ \frac{15}{2}\rho_1^3 \cos(\theta_2 - \theta_1) + 5\rho_1^3 \sin(\theta_2 - \theta_1) \\ &+ \frac{15}{2}\rho_1^2\rho_2 \sin 2(\theta_2 - \theta_1) + 6\rho_1^2\rho_2 \cos 2(\theta_2 - \theta_1).\end{aligned} \tag{94}$$

6.1. BIFURCATION ANALYSIS

It is seen from equation (94) that only three of the four equations are independent. So $\phi = \theta_2 - \theta_1$, then we have

$$\frac{\mathrm{d}\rho_1}{\mathrm{d}\tau} = \rho_2 \cos\phi,$$

$$\frac{\mathrm{d}\rho_2}{\mathrm{d}\tau} = -\frac{1}{4}\mu_1\rho_2 - \frac{3}{2}\mu_2\rho_2 - \frac{1}{4}\mu_1\rho_1 \sin\phi + 15\rho_1^2\rho_2 + 30\rho_1\rho_2^2 \sin\phi - 80\rho_1\rho_2^2 \cos\phi$$
$$+ \frac{15}{2}\rho_1^3 \sin\phi - 5\rho_1^3 \cos\phi + 6\rho_1^2\rho_2 \sin 2\phi - \frac{15}{2}\rho_1^2\rho_2 \cos 2\phi,$$

$$\frac{\mathrm{d}\phi}{\mathrm{d}\tau} = -\frac{1}{4}\mu_1\frac{\rho_1}{\rho_2}\cos\phi - \frac{\rho_2}{\rho_1}\sin\phi - 22\rho_1^2 + \frac{15}{2}\rho_1^2 \sin 2\phi - 10\rho_1^2 \cos 2\phi$$
$$+ 30\rho_1\rho_2 \cos\phi + 80\rho_1\rho_2 \sin\phi + \frac{15}{2}\frac{\rho_1^3}{\rho_2}\cos\phi + 5\frac{\rho_1^3}{\rho_2}\sin\phi. \tag{95}$$

Note that, unlike the non-resonant case, although the trivial solution $\rho_1 = \rho_2 = 0$ (which represents the initial equilibrium $x_i = 0$ or $z_i = 0$) can be obtained from equation (94), its stability cannot be determined from equation (94) or equation (95). However, based on equation (92), one may use linearization to find the characteristic polynomial evaluated on the initial equilibrium, given by

$$P(\lambda) = \lambda^4 + \left(\frac{1}{2}\mu_1 + 3\mu_2\right)\lambda^3 + \left(2 + \frac{1}{2}\mu_1\mu_2\right)\lambda^2 + \left(3\mu_2 - \frac{1}{2}\mu_1\right)\lambda + 1. \tag{96}$$

Using the stability conditions given in equation (11) and noticing that $\mu_1 \geqslant 0$, $\mu_2 \geqslant 0$ yields

$$\mu_2\mu_1^2 + 8\mu_1 - 36\mu_2^3 < 0 \tag{97}$$

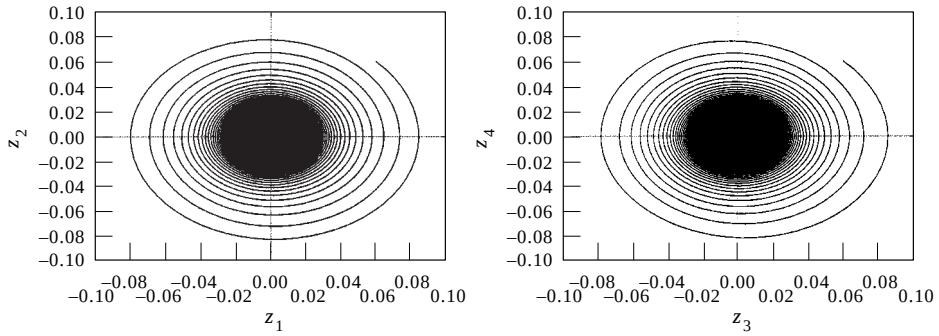

Figure 18. Trajectory starting from $(z_1, z_2, z_3, z_4) = (0{\cdot}06, 0{\cdot}06, 0{\cdot}06, 0{\cdot}06)$ converges to the E.S. when $(\mu_1, \mu_2) = (0{\cdot}03, 0{\cdot}2)$.

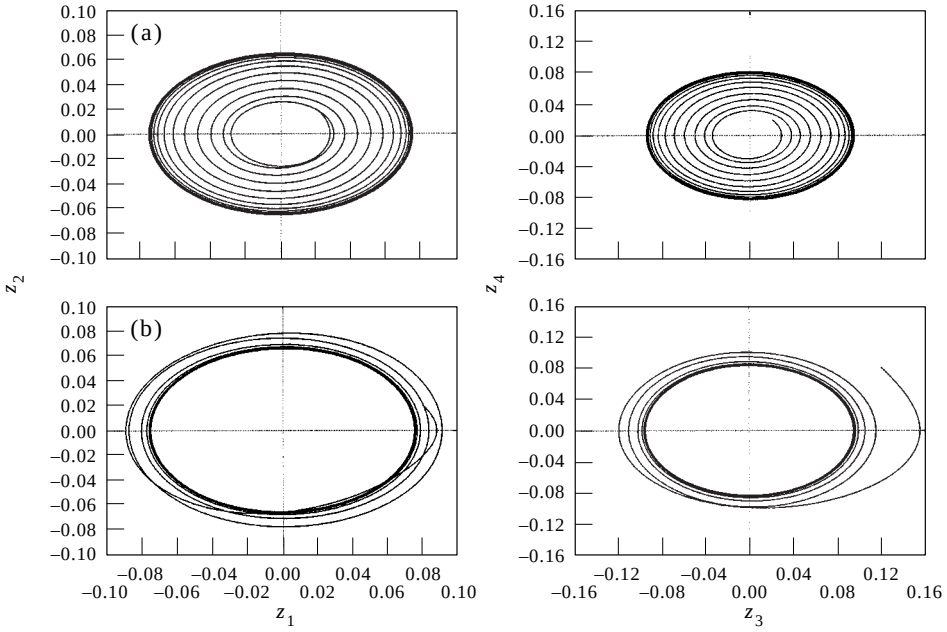

Figure 19. Phase-locked periodic solutions: (a) starting from $(z_1, z_2, z_3, z_4) = (0{\cdot}02, 0{\cdot}02, 0{\cdot}02, 0{\cdot}02)$.

which, in turn, results in

$$0 \leqslant \mu_1 < \frac{4}{\mu_2}\left[-1 + \sqrt{1 + \frac{9}{4}\mu_2^4}\right] \approx \frac{9}{2}\mu_2^3. \tag{98}$$

Thus, when $0 < \mu_1 < (9/2)\mu_2^3$, the initial equilibrium $x_i = 0$ is stable. When the parameters μ_1 and μ_2 are varied such that the critical boundary

$$L: \qquad \mu_1 = \frac{9}{2}\mu_2^3 \tag{99}$$

is reached, the initial equilibrium becomes unstable and phase-locked periodic solutions bifurcate from the boundary. The bifurcation diagram is given in Figure 17.

Letting $\mathrm{d}\rho_1/\mathrm{d}\tau = \mathrm{d}\rho_2/\mathrm{d}\tau = \mathrm{d}\phi/\mathrm{d}\tau = 0$ yields the algebraic equations which can be used for solving possible phase-locked periodic solutions. No closed form solutions can be obtained from these non-linear algebraic equations. However, we may find all the possible periodic solutions by the following procedure. First, note from the first of equations (95) that $\mathrm{d}\rho_1/\mathrm{d}\tau = 0$ leads to $\cos\phi = 0$ (since $\rho_2 \neq 0$) which yields two possibilities: $\phi = \pm\frac{1}{2}\pi$ (for $-\pi < \phi \leqslant \pi$), or $\sin\phi = \pm 1$. Substituting $\phi = \pi/2$ into the remaining two algebraic equations gives

$$\begin{aligned} \mu_1\rho_1 + (\mu_1 + 6\mu_2)\rho_2 - 30\rho_1^3 - 90\rho_1^2\rho_2 - 120\rho_1\rho_2^2 = 0, \\ \rho_2^2 - 5\rho_1^4 + 28\rho_1^3\rho_2 - 80\rho_1^2\rho_2^2 = 0, \end{aligned} \tag{100}$$

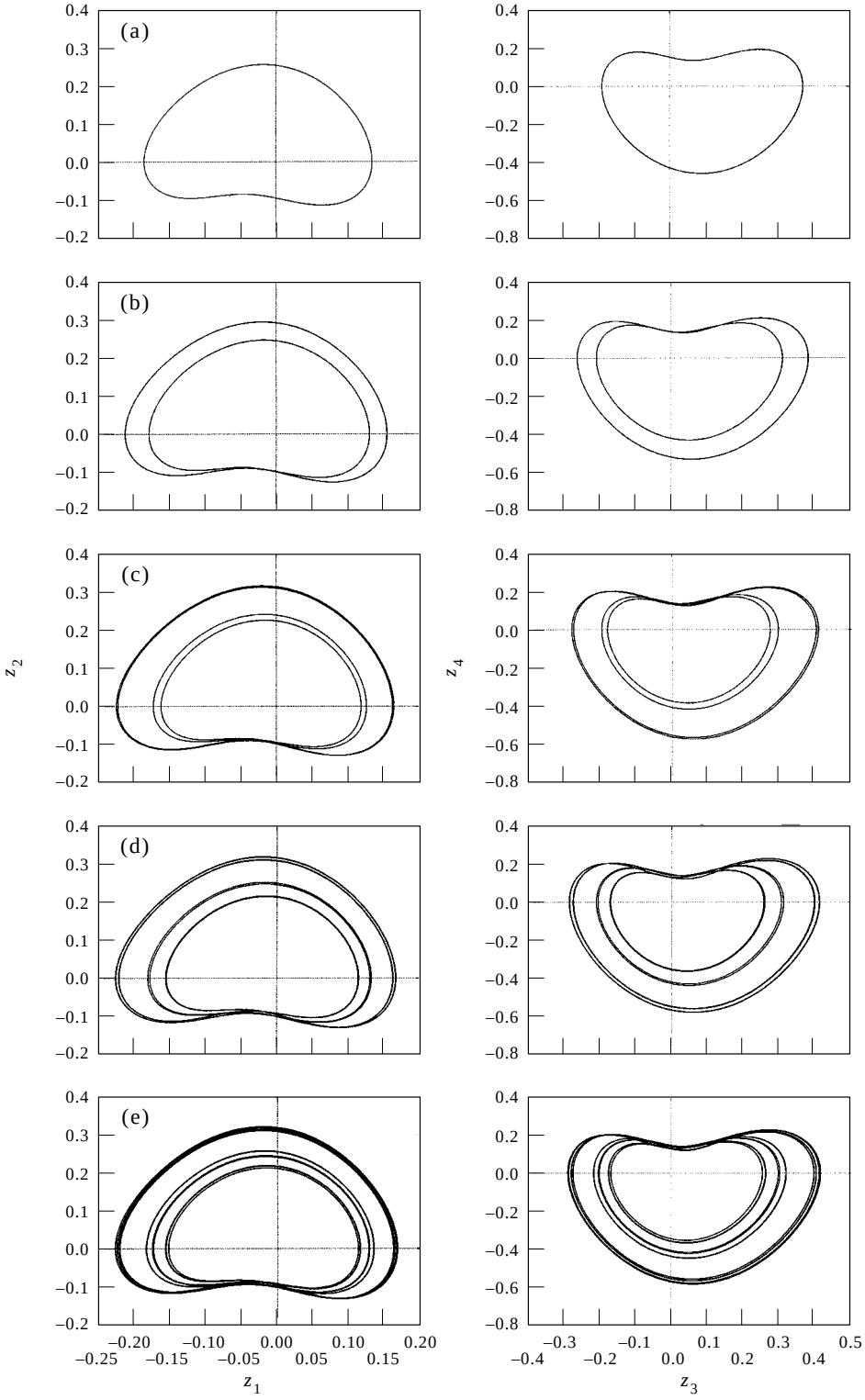

Figure 20(a–e).

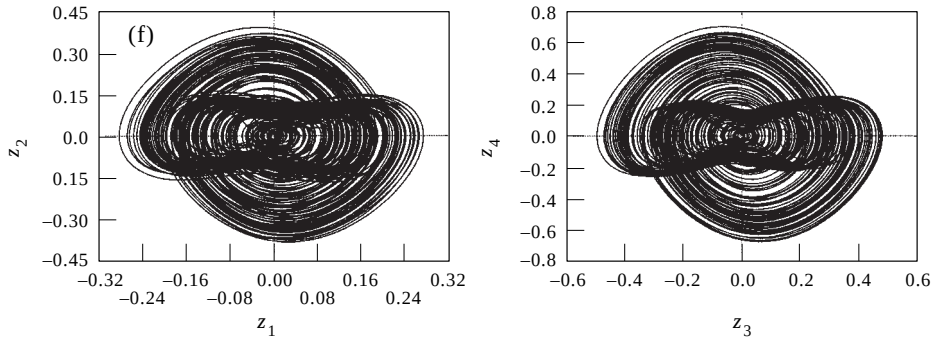

Figure 20(f).

Figure 20. Period-doubling to chaos for $(\mu_1, \mu_2) = (0{\cdot}1, 0{\cdot}1)$ when $\Omega = 1{\cdot}0$ with initial condition $(z_1, z_2, z_3, z_4) = (-0{\cdot}05, 0{\cdot}0, -0{\cdot}05, 0{\cdot}0)$; (a) $\alpha = 1{\cdot}05$, period-1; (b) $\alpha = 1{\cdot}08$, period-2; (c) $\alpha = 1{\cdot}095$, period-4; (d) $\alpha = 1{\cdot}0989$, period-8; (e) $\alpha = 1{\cdot}0999$, period-16; (f) $\alpha = 1{\cdot}109$, chaos.

from which one may eliminate (e.g., by using a symbolic computation language Maple) variable ρ_2 to obtain a polynomial for ρ_1:

$$16\,862\,400\rho_1^8 - 224\,100\rho_1^6 + 900\rho_1^4 - 60\mu_1\rho_1^2 + \mu_1^2 = 0 \tag{101}$$

in which all the coefficients have been taken the leading term (first order approximation) and then ρ_2 is given by

$$\rho_2 = -\frac{\rho_1(1800\rho_1^4 - 30\rho_1^2 + \mu_1)}{10\,560\rho_1^4 - 90\rho_1^2 + \mu_1 + 6\mu_2}. \tag{102}$$

Now, given the values of μ_1 and μ_2, equation (101) can be used to numerically find all possible (stable and unstable) periodic solutions ($\rho_1 > 0$) and then $\rho_2(>0)$ is determined from equation (102).

The solutions for the case of $\phi = -\pi/2$ can be similarly found. The stability conditions for these phase-locked periodic solutions are straightforwardly determined from the Jacobian matrix of equation (95).

6.2. NUMERICAL RESULTS

By choosing $(\mu_1, \mu_2) = (0{\cdot}03, 0{\cdot}2)$, which represents a point in the parameter space (see the black circle dots in Figure 17) located in the stable region for the E.S., one can use time integration to find a numerical solution shown in Figure 18. The trajectory starting from the initial point $(z_1, z_2, z_3, z_4) = (0{\cdot}06, 0{\cdot}06, 0{\cdot}06, 0{\cdot}06)$ converges to the origin—the initial equilibrium of the system.

If the parameters are chosen as $\mu_1 = \mu_2 = 0{\cdot}2$, then use the analytic formulas given in section 6.1 and a simple approach for solving polynomials to obtain the following solutions:

$$\begin{aligned} &\rho_1 = 0{\cdot}0606, \quad \rho_2 = -0{\cdot}0057; \qquad \rho_1 = 0{\cdot}1112, \quad \rho_2 = -0{\cdot}0061; \qquad \text{for } \phi = +\pi/2 \\ &\rho_1 = 0{\cdot}0606, \quad \rho_2 = 0{\cdot}0057; \qquad \rho_1 = 0{\cdot}1112, \quad \rho_2 = 0{\cdot}0061; \qquad \text{for } \phi = -\pi/2. \end{aligned} \tag{103}$$

Taking the positive value yields two solutions when $\phi = -\pi/2$. Next substituting the two solutions into the Jacobian matrix of equation (95) shows that the first solution is stable while the second solution is unstable. Thus, we have the following results:

$$\begin{aligned} &\text{solution} \quad \rho_1 = 0{\cdot}0606, \quad \rho_2 = 0{\cdot}0057, \quad \phi = -\pi/2 \quad \text{is stable;} \\ &\text{solution} \quad \rho_1 = 0{\cdot}1112, \quad \rho_2 = 0{\cdot}0061, \quad \phi = -\pi/2 \quad \text{is unstable.} \end{aligned} \tag{104}$$

Similarly, apply the linear transformation (91) and the non-linear transformation given by equations (B9)–(B12) in Appendix B to obtain

$$z_1 = 0{\cdot}0038, \quad z_2 = -0{\cdot}0573, \quad z_3 = 0{\cdot}0108, \quad z_4 = -0{\cdot}0697 \tag{105}$$

which yields the analytic prediction $\sqrt{z_1^2 + z_2^2} = 0{\cdot}0574$ and $\sqrt{z_3^2 + z_4^2} = 0{\cdot}0705$.

By a time integration scheme, one can find the numerical solution for $\mu_1 = \mu_2 = 0{\cdot}2$, shown in Figure 19 from which the amplitude of the phase-locked periodic solution can be estimated as

$$\sqrt{z_1^2 + z_2^2} = 0{\cdot}065, \quad \sqrt{z_3^2 + z_4^2} = 0{\cdot}080 \tag{106}$$

which closes to the analytic prediction.

Furthermore, by numerically exploring the phase-locked periodic solutions using equations (95), (101) and (102), we have found that one of the two solutions is always unstable in the region bounded by the critical line L and the positive μ_1-axis. the other periodic solution is stable in the region except for the small region bounded by the dotted curve.

7. CHAOS

Finally, in this section, we shall, based on the numerical approach, investigate the possibility of system (7) having chaotic motions. Here, the force P_2 (i.e., f_5) is modified from a constant to a periodic function

$$f_5 = 2 + \alpha \cos(\Omega\tau), \tag{107}$$

so that the system now becomes a non-autonomous system. Furthermore, the system parameters are chosen as

$$f_1 = 4, \quad f_2 = 1, \quad f_3 = 2, \quad f_4 = 0, \quad f_6 = f_7 = 0, \quad \eta_1 = 0, \quad \eta_2 = 0, \tag{108}$$

such that the linearized system without the forcing term has two repeated pairs of purely imaginary eigenvalues $\lambda_{1,2} = \lambda_{3,4} = \pm i$, evaluated at the critical point $\eta_1 = \eta_2 = 0$.

Based on the original differential equation (7), a time integration scheme has been employed to find double-periodic motions leading to chaos—a well-known chaos scenario. The cascading bifurcations happens when the external frequency, Ω, is chosen close to 1 (here it is 1·05) and increasing the amplitude of the forcing

term, α, from 1. When $\alpha < 1{\cdot}08$, the numerical result shows a stable period-1 motion (see Figure 20(a)). When $\alpha = 1{\cdot}08$, the period-1 motion becomes unstable and bifurcates into a period-2 motion (Figure 20(b)), which is stable until α equals 1·095 at which the period-2 motion becomes unstable and bifurcates into a period-4 motion (Figure 20(c)). This cascading bifurcation continues to occur at $\alpha = 1{\cdot}0989$ leading to period-8 motion (Figure 20(d)) and at $\alpha = 1{\cdot}0999$ to period-16 motion (Figure 20(e)). Finally, the motion becomes chaotic at $\alpha = 1{\cdot}109$, which is shown in Figure 20(f).

It should be noted that the trajectories shown in Figure 20 are actually the projections of the trajectories in the four-dimensional state space onto the z_1–z_2 and z_3–z_4 sub-spaces. Also note that the transient trajectories starting from the initial point $(z_1, z_2, z_3, z_4) = (0{\cdot}05, 0{\cdot}0, 0{\cdot}05, 0{\cdot}0)$ have been omitted in Figure 20 in order to give a clear visualization. It is seen from Figure 20(f) that the trajectories are symmetric with respect to the origin. This is because if we replace z_i by $-z_i$ in equation (7), the system does not change. In fact, this also happens to all parts (a)–(e) in Figure 20—if the initial point is chosen as $(z_1, z_2, z_3, z_4) = (-0{\cdot}05, 0{\cdot}0, -0{\cdot}05, 0{\cdot}0)$, then another period-doubling cascading bifurcation leading to chaos would be obtained. The chaotic motion travels along the seemingly random orbits, but bounded and never repeated.

8. CONCLUSIONS

A simple physical system—double pendulum has been studied in detail to show a rich dynamic behaviour of the system in the vicinity of a number of compound critical points. Closed form solutions have been obtained, via bifurcation analysis, for periodic and quasi-periodic solutions. The stability conditions for the steady state solutions are also given explicitly in terms of the system parameters. Critical stability boundaries along which incipient, secondary and tertiary bifurcations leading to periodic solutions, quasi-periodic motions on 2-D and 3-D tori are also explicitly obtained. All the derivations are simple and straightforward with the aid of normal form theory. Numerical computations have been performed for each of the bifurcation cases and shown that all numerical solutions agree with the analytic predictions, at least qualitatively. It has been found that an analytic approach can provide a general picture of dynamic behaviour of a non-linear system in the vicinity of a critical point and then numerical computations can be purposely performed to get more accurate results. This suggests that it is necessary to use both analytical and numerical methods for the study of non-linear systems. A numerical approach has also been applied to find cascading bifurcations leading to chaos for certain parameter values.

ACKNOWLEDGMENTS

The authors gratefully acknowledge the support of the Natural Sciences and Engineering Research Council of Canada. Q. B. also would like to acknowledge partial support received from the China Scholarship Council (CSC).

REFERENCES

1. J. Guckenheimer and P. Holmes 1983 *Nonlinear Oscillations, Dynamical Systems, and Bifurcations of Vector Fields*. New York: Springer-Verlag.
2. P. Yu and K. Huseyin 1986 *Dynamics and Stability of Systems* **1**, 73–86. Static and dynamic bifurcations associated with a double zero eigenvalues.
3. W. F. Langford 1979 *SIAM Journal of Applied Mathematics* **37**, 22–48. Periodic and steady mode interactions lead to tori.
4. P. Yu and K. Huseyin 1988 *IEEE Transactions of Automatic Control* **33**, 28–41. A perturbation analysis of interactive static and dynamic bifurcations.
5. K. Huseyin and P. Yu 1988 *Applied Mathematical Modelling* **12**, 189–201. On bifurcations into nonresonant quasi-periodic motions.
6. P. Yu and K. Huseyin 1993 *Quarterly Applied Mathematics* **51**, 91–100. On phase-locked motions associated with strong resonance.
7. V. Mandadi and K. Huseyin 1980 *International Journal of Non-linear Mechanics* **15**, 159–172. Non-linear bifurcation analysis of non-gradient systems.
8. K. Huseyin 1986 *Multiple-Parameter Stability Theory and Its Applications*. Oxford: Oxford University Press.
9. R. Scheidl, H. Troger and K. Zeman 1984 *International Journal of Non-linear Mechanics* **19**, 163–176. Coupled flutter and divergence bifurcation of a double pendulum.
10. S. Samaranayake and A. K. Bajaj 1993 *Nonlinear Dynamics* **4**, 605–633. Bifurcation in the dynamics of an orthogonal double pendulum.
11. D. E. Gilsinn 1993 *Nonlinear Dynamics* **4**, 289–308. Constructing invariant tori for two weakly coupled van der Pol oscillators.
12. P. Steen and S. H. Davis 1982 *SIAM Journal of Applied Mathematics* **42**, 1345–1368. Quasi-periodic bifurcation in non-linearly coupled oscillators near a point of strong resonance.
13. L. Jezequel and C. H. Lamarque 1991 *Journal of Sound and Vibration* **149**, 429–459. Analysis of non-linear dynamical systems by the normal form theory.
14. Z. C. Feng and P. R. Sethna 1990 *Dynamics and Stability of Systems* **5**, 201–226. Global bifurcation and chaos in parametrically forced systems with one-one resonance.
15. R. H. Rand and P. J. Holmes 1980 *International Journal of Non-linear Mechanics* **15**, 387–399. Bifurcation of periodic motions in two weakly coupled van der Pol oscillators.
16. S. Foale and J. M. T. Thompson 1991 *Comp. Mathematics in Applied Mechanical Engineering* **89**, 381–394. Geometrical concepts and computational techniques of non-linear dynamics.
17. S. A. van Gils, M. P. Krupa and W. F. Langford 1990 *Nonlinearity* **3**, 1–26. Hopf bifurcation with non-semisimple 1:1 resonance.
18. Y. S. Chen and Q. C. Zhang 1990 *Acta Mechanica Sinica* **22**, 413–419. A new method for solving asymptotic solution of non-linear vibration system—simple method for computing normal form of vector field.
19. S. N. Chow, C. Z. Li and D. Wang 1994 *Normal Forms and Bifurcation of Planar Vector Fields*. Cambridge: Cambridge University Press.
20. K. Ogata 1970 *Modern Control Engineering*. Englewood Cliffs, NJ: Prentice-Hall.
21. J. Carr 1981 *Applications of Center Manifold Theory*. AMS 35, New York: Springer-Verlag.
22. G. Iooss and M. Adelmeyer 1992 *Topics in Bifurcation Theory and Applications*. Singapore: World Scientific.

APPENDIX A: NON-LINEAR FUNCTIONS

The non-linear functions Nf_i, $i = 1, 2, 3, 4$ in equation (16) are given below.

$$\begin{aligned} Nf_1 = {} & \frac{330\,733}{33\,957}\,x_1^3 + \frac{275\,353\,739}{69\,883\,506}\,x_2^3 - \frac{145\,693}{32\,076}\,x_3^3 - \frac{237\,755}{396}\,x_4^3 \\ & + \frac{6\,593\,768}{237\,699}\,x_1^2x_2 - \frac{377\,075}{14\,553}\,x_1^2x_3 - \frac{74\,260}{1617}\,x_1^2x_4 + \frac{33\,961\,273}{1\,663\,893}\,x_1x_2^2 \\ & - \frac{7\,014\,439}{259\,308}\,x_2^2x_3 - \frac{2\,155\,859}{9702}\,x_2^2x_4 + \frac{37\,343}{2079}\,x_1x_3^2 \\ & + \frac{1\,832\,321}{87\,318}\,x_2x_3^2 - \frac{25\,403}{1188}\,x_3^2x_4 - \frac{20\,296}{77}\,x_1x_4^2 \\ & - \frac{52\,650\,701}{950\,796}\,x_2x_4^2 + \frac{50\,095}{1188}\,x_3x_4^2 - \frac{5\,861\,071}{101\,871}\,x_1x_2x_3 \\ & - \frac{2\,748\,695}{33\,957}\,x_1x_2x_4 + \frac{62\,852}{2079}\,x_1x_3x_4 - \frac{34\,570}{14\,553}\,x_2x_3x_4, \end{aligned} \tag{A1}$$

$$\begin{aligned} Nf_2 = {} & -\frac{5108}{1617}\,x_1^3 - \frac{1\,423\,276}{1\,663\,893}\,x_2^3 + \frac{3955}{2673}\,x_3^3 + \frac{1519}{6}\,x_4^3 - \frac{103\,856}{11\,319}\,x_1^2x_2 + \frac{6080}{693}\,x_1^2x_3 \\ & + \frac{1566}{77}\,x_1^2x_4 - \frac{489\,232}{79\,233}\,x_1x_2^2 + \frac{333\,026}{33\,957}\,x_2^2x_3 + \frac{534\,139}{22\,638}\,x_2^2x_4 - \frac{194}{33}\,x_1x_3^2 \\ & - \frac{15\,475}{2079}\,x_2x_3^2 + \frac{2009}{198}\,x_3^2x_4 + \frac{1238}{11}\,x_1x_4^2 + \frac{20\,743}{231}\,x_2x_4^2 - \frac{203}{9}\,x_3x_4^2 \\ & + \frac{100\,300}{4851}\,x_1x_2x_3 + \frac{55\,406}{1617}\,x_1x_2x_4 - \frac{1502}{99}\,x_1x_3x_4 + \frac{355}{693}\,x_2x_3x_4, \end{aligned} \tag{A2}$$

$$\begin{aligned} Nf_3 = {} & \frac{4769}{539}\,x_1^3 + \frac{1\,505\,233}{369\,754}\,x_2^3 - \frac{1631}{396}\,x_3^3 - \frac{21\,007}{44}\,x_4^3 + \frac{94\,296}{3773}\,x_1^2x_2 - \frac{12\,455}{539}\,x_1^2x_3 \\ & - \frac{1734}{49}\,x_1^2x_4 + \frac{503\,385}{26\,411}\,x_1x_2^2 - \frac{2\,468\,993}{105\,644}\,x_2^2x_3 - \frac{4\,621\,917}{105\,644}\,x_2^2x_4 + \frac{3755}{231}\,x_1x_3^2 \\ & + \frac{59\,251}{3234}\,x_2x_3^2 - \frac{2071}{132}\,x_3^2x_4 - \frac{16\,014}{77}\,x_1x_4^2 - \frac{195\,375}{1078}\,x_2x_4^2 + \frac{1231}{44}\,x_3x_4^2 \\ & - \frac{188\,351}{3773}\,x_1x_2x_3 - \frac{242\,283}{3773}\,x_1x_2x_4 + \frac{1634}{77}\,x_1x_3x_4 - \frac{1325}{539}\,x_2x_3x_4, \end{aligned} \tag{A3}$$

$$
\begin{aligned}
Nf_4 = &-\frac{38\,491}{33\,957}x_1^3 - \frac{34\,456\,445}{69\,883\,506}x_2^3 + \frac{16\,939}{32\,076}x_3^3 + \frac{25\,781}{396}x_4^3 - \frac{69\,448}{21\,609}x_1^2x_2 \\
&+\frac{43\,445}{14\,553}x_1^2x_3 + \frac{1132}{231}x_1^2x_4 - \frac{4\,012\,927}{1\,663\,893}x_1x_2^2 + \frac{8\,739\,083}{2\,852\,388}x_2^2x_3 \\
&+\frac{812\,885}{135\,828}x_2^2x_4 - \frac{4337}{2079}x_1x_3^2 - \frac{18\,973}{7938}x_2x_3^2 + \frac{2645}{1188}x_3^2x_4 + \frac{2192}{77}x_1x_4^2 \\
&+\frac{236\,861}{9702}x_2x_4^2 - \frac{4969}{1188}x_3x_4^2 + \frac{665\,353}{101\,871}x_1x_2x_3 + \frac{42\,527}{4851}x_1x_2x_4 \\
&-\frac{6404}{2079}x_1x_3x_4 + \frac{4330}{14\,553}x_2x_3x_4. \qquad \text{(A4)}
\end{aligned}
$$

The non-linear functions Ng_i, $i = 1, 2, 3, 4$ in equation (34) are given by

$$
\begin{aligned}
Ng_1 = &-\frac{635}{1152}x_1^3 - \frac{146\,345}{1008}x_2^3 + \frac{703}{63}\sqrt{6}x_3^3 + \frac{99\,723\,742}{44\,217}x_4^3 + \frac{889}{192}x_1^2x_2 \\
&-\frac{25}{16}\sqrt{6}x_1^2x_3 - \frac{54\,133}{1632}x_1^2x_4 - \frac{739}{96}x_1x_2^2 + \frac{8315}{84}\sqrt{6}x_2^2x_3 \\
&+\frac{427\,495}{408}x_4x_2^2 - 12x_1x_3^2 - \frac{872}{7}x_2x_3^2 + \frac{12\,881}{34}x_4x_3^2 - \frac{4\,995\,415}{55\,488}x_1x_4^2 \\
&-\frac{73\,595\,179}{27\,744}x_2x_4^2 + \frac{9\,172\,643}{13\,872}\sqrt{6}x_3x_4^2 + \frac{113}{12}\sqrt{6}x_1x_2x_3 - \frac{679}{408}x_1x_2x_4 \\
&-\frac{2129}{51}\sqrt{6}x_1x_3x_4 - \frac{26\,513}{51}\sqrt{6}x_2x_3x_4, \qquad \text{(A5)}
\end{aligned}
$$

$$
\begin{aligned}
Ng_2 = &\frac{52\,507}{23\,808}x_1^3 - \frac{9547}{480}x_2^3 + \frac{12\,883}{930}\sqrt{6}x_3^3 + \frac{2\,967\,447\,847}{9\,138\,180}x_4^3 - \frac{24\,829}{19\,840}x_1^2x_2 \\
&+\frac{6895}{992}\sqrt{6}x_1^2x_3 + \frac{1\,078\,693}{168\,640}x_1^2x_4 + \frac{12\,047}{9920}x_1x_2^2 + \frac{4311}{248}\sqrt{6}x_2^2x_3 \\
&+\frac{6\,536\,089}{42\,160}x_2^2x_4 + \frac{6251}{155}x_1x_3^2 - \frac{4242}{155}x_2x_3^2 + \frac{150\,605}{2108}x_3^2x_4 \\
&+\frac{70\,804\,699}{5\,733\,760}x_1x_4^2 - \frac{1\,196\,764\,961}{2\,866\,880}x_2x_4^2 + \frac{135\,359\,273}{1\,433\,440}\sqrt{6}x_3x_4^2 \\
&-\frac{1169}{1240}\sqrt{6}x_1x_2x_3 - \frac{508\,193}{42\,160}x_1x_2x_4 + \frac{29\,638}{2635}\sqrt{6}x_1x_3x_4 \\
&-\frac{468\,349}{5270}\sqrt{6}x_2x_3x_4, \qquad \text{(A6)}
\end{aligned}
$$

$$
\begin{aligned}
Ng_3 = {} & \frac{19\,159}{35\,712}\sqrt{6}x_1^3 + \frac{2081}{720}\sqrt{6}x_2^3 + \frac{2434}{155}x_3^3 - \frac{4\,525\,321\,843}{109\,658\,160}\sqrt{6}x_4^3 \\
& - \frac{15\,673}{29\,760}\sqrt{6}x_1^2x_2 + \frac{5005}{496}x_1^2x_3 \\
& + \frac{1\,609\,307}{505\,920}\sqrt{6}x_1^2x_4 + \frac{3353}{4960}\sqrt{6}x_1x_2^2 - \frac{811}{124}x_2^2x_3 - \frac{767\,823}{42\,160}\sqrt{6}x_2^2x_4 \\
& + \frac{18\,431}{1860}\sqrt{6}x_1x_3^2 + \frac{33}{310}\sqrt{6}x_2x_3^2 - \frac{9611}{3162}\sqrt{6}x_3^2x_4 \\
& + \frac{32\,161\,199}{4\,300\,320}\sqrt{6}x_1x_4^2 + \frac{86\,775\,059}{2\,150\,160}\sqrt{6}x_2x_4^2 - \frac{13\,200\,117}{179\,180}x_3x_4^2 \\
& - \frac{2611}{620}x_1x_2x_3 - \frac{340\,417}{126\,480}\sqrt{6}x_1x_2x_4 + \frac{17\,633}{620}x_1x_3x_4 \\
& + \frac{198\,653}{5270}x_2x_3x_4, \qquad \text{(A7)}
\end{aligned}
$$

$$
\begin{aligned}
Ng_4 = {} & -\frac{34\,459}{8928}x_1^3 + \frac{233\,053}{1260}x_2^3 - \frac{379\,508}{9765}\sqrt{6}x_3^3 - \frac{2\,342\,159\,033}{806\,310}x_4^3 \\
& - \frac{15\,827}{7440}x_1^2x_2 - \frac{765}{62}x_1^2x_3 + \frac{37\,901}{1860}x_1^2x_4 + \frac{19\,601}{3720}x_1x_2^2 \\
& - \frac{87\,074}{651}\sqrt{6}x_2^2x_3 - \frac{631\,397}{465}x_2^2x_4 - \frac{10\,642}{155}x_1x_3^2 \\
& + \frac{194\,548}{1085}x_2x_3^2 - \frac{16\,174}{31}x_3^2x_4 + \frac{8\,262\,871}{126\,480}x_1x_4^2 + \frac{220\,552\,171}{63\,240}x_2x_4^2 \\
& - \frac{26\,879\,963}{31\,620}\sqrt{6}x_3x_4^2 - \frac{3502}{465}\sqrt{6}x_1x_2x_3 + \frac{11\,984}{465}x_1x_2x_4 \\
& + \frac{8951}{465}\sqrt{6}x_1x_3x_4 + \frac{324\,386}{465}\sqrt{6}x_2x_3x_4. \qquad \text{(A8)}
\end{aligned}
$$

The non-linear functions Nh_i, $i = 1, 2$ in equation (67) are

$$
\begin{aligned}
Nh_1 = {} & \frac{351\,167}{2\,765\,952}x_1^3 - \frac{625}{4116}x_2^3 + \frac{286\,595}{1\,229\,312}\sqrt{2}x_3^3 - \frac{1215}{1372}x_4^3 + \frac{753\,923}{1\,843\,968}\sqrt{2}x_1^2x_3 \\
& + \frac{48\,575}{24\,696}x_1x_2^2 + \frac{9715}{5488}\sqrt{2}x_2^2x_3 - \frac{1125}{1372}x_2^2x_4 + \frac{478\,909}{614\,656}x_1x_3^2 + \frac{4215}{2744}x_1x_4^2 \\
& - \frac{2025}{1372}x_2x_4^2 + \frac{7587}{5488}\sqrt{2}x_3x_4^2 + \frac{14\,165}{4166}x_1x_2x_4 + \frac{8499}{2744}\sqrt{2}x_2x_3x_4, \qquad \text{(A9)}
\end{aligned}
$$

$$Nh_2 = -\frac{3\,568\,499}{24\,893\,568}x_1^3 + \frac{6625}{37\,044}x_2^3 - \frac{1\,015\,277}{3\,687\,936}\sqrt{2}x_3^3 + \frac{1431}{1372}x_4^3$$

$$-\frac{2\,628\,781}{5\,531\,904}\sqrt{2}x_1^2x_3 - \frac{56\,635}{24\,696}x_1x_2^2 - \frac{11\,327}{5488}\sqrt{2}x_2^2x_3 + \frac{1325}{1372}x_2^2x_4$$

$$-\frac{562\,705}{614\,656}x_1x_3^2 - \frac{14\,585}{8232}x_1x_4^2 + \frac{2385}{1372}x_2x_4^2 - \frac{8751}{5488}\sqrt{2}x_3x_4^2$$

$$-\frac{5475}{1372}x_1x_2x_4 - \frac{9855}{2744}\sqrt{2}x_2x_3x_4. \tag{A10}$$

APPENDIX B: NON-LINEAR TRANSFORMATIONS

The non-linear transformations between the co-ordinates x_i and the normal form co-ordinates y_i for the case of one simple zero and a pair of purely imaginary eigenvalues are given as follows.

$$x_1 = y_1 + \left(\frac{3}{14}\mu_2 - \frac{3}{2}\mu_1\right)y_2 + \sqrt{6}\left(\frac{27}{56}\mu_2 + \frac{3}{8}\mu_1\right)y_3 - \frac{4367}{36}y_2^3 - \frac{209\,129}{3024}\sqrt{6}y_3^3$$

$$+\frac{75}{16}y_1^2y_2 + \frac{889}{384}\sqrt{6}y_1^2y_3 - \frac{113}{16}y_1y_2^2 - \frac{146\,345}{2016}\sqrt{6}y_2^2y_3 + \frac{113}{16}y_1y_3^2$$

$$-\frac{703}{21}y_2y_3^2 + \frac{413}{384}\sqrt{6}y_1y_2y_3, \tag{B1}$$

$$x_2 = y_2 + \left(\frac{189}{620}\mu_1 - \frac{3}{155}\mu_2\right)y_1 + \left(\frac{423}{2480}\mu_1 - \frac{219}{2480}\mu_2\right)y_2 + \sqrt{6}\left(\frac{171}{9920}\mu_1\right.$$

$$\left.-\frac{603}{9920}\mu_2\right)y_3 - \frac{19\,159}{11\,904}y_1^3 - \frac{3\,197\,209}{238\,080}y_2^3 - \frac{1\,266\,797}{317\,440}\sqrt{6}y_3^3 - \frac{6167}{1280}y_1^2y_2$$

$$-\frac{7259}{5120}\sqrt{6}y_1^2y_3 - \frac{290\,927}{14\,880}y_1y_2^2 - \frac{1\,263\,009}{317\,440}\sqrt{6}y_2^2y_3 - \frac{90\,797}{7440}y_1y_3^2$$

$$-\frac{833\,391}{79\,360}y_2y_3^2 - \frac{81\,781}{5952}\sqrt{6}y_1y_2y_3, \tag{B2}$$

$$x_3 = y_3 - \sqrt{6}\left(\frac{609}{4960}\,\mu_1 - \frac{297}{4960}\,\mu_2\right)y_1 + \sqrt{6}\left(\frac{171}{9920}\,\mu_1 - \frac{603}{9920}\,\mu_2\right)y_2 - \left(\frac{423}{2480}\,\mu_1 - \frac{219}{2480}\,\mu_2\right)y_3 + \frac{52\,507}{47\,616}\sqrt{6}y_1^3 - \frac{2\,915\,873}{952\,320}\sqrt{6}y_2^3 + \frac{971\,781}{79\,360}\,y_3^3 - \frac{7259}{5120}\sqrt{6}y_1^2y_2 + \frac{6167}{1280}\,y_1^2y_3 + \frac{853\,951}{59\,520}\sqrt{6}y_1y_2^2 + \frac{1\,115\,257}{79\,360}\,y_2^2y_3 + \frac{191\,191}{29\,760}\sqrt{6}y_1y_3^2 - \frac{2\,147\,527}{317\,440}\sqrt{6}y_2y_3^2 - \frac{26\,075}{1488}\,y_1y_2y_3, \tag{B3}$$

$$x_4 = -\left(\frac{17}{155}\,\mu_1 + \frac{1411}{7595}\,\mu_2\right)y_1 - \left(\frac{1326}{24\,025}\,\mu_1 + \frac{3774}{33\,635}\,\mu_2\right)y_2 - \sqrt{6}\left(\frac{1632}{24\,025}\,\mu_1 + \frac{3672}{33\,635}\,\mu_2\right)y_3 - \frac{34\,459}{31\,248}\,y_1^3 + \frac{2\,130\,802\,049}{31\,568\,850}\,y_2^3 - \frac{856\,323\,592}{110\,490\,975}\sqrt{6}y_3^3 + \frac{256\,411}{192\,200}\,y_1^2y_2 - \frac{979\,727}{288\,300}\sqrt{6}y_1^2y_3 + \frac{2\,149\,191}{221\,960}\,y_1y_2^2 - \frac{944\,269\,369}{36\,830\,325}\sqrt{6}y_2^2y_3 - \frac{2\,149\,191}{221\,960}\,y_1y_3^2 + \frac{1\,297\,000\,448}{36\,830\,325}\,y_2y_3^2 + \frac{25\,585}{16\,647}\sqrt{6}y_1y_2y_3. \tag{B4}$$

The non-linear transformations for the case of two pairs of purely imaginary eigenvalues (non-resonance) between the co-ordinates x_i and the normal form co-ordinates y_i are given by

$$x_1 = y_1 + \left(\frac{11}{14}\,\mu_1 - \frac{75}{112}\,\mu_2\right)y_2 + \sqrt{2}\left(\frac{33}{14}\,\mu_1 - \frac{135}{28}\,\mu_2\right)y_4 - \frac{28\,255\,501}{22\,127\,616}\,y_1^3 + \frac{625}{10\,976}\,y_2^3 - \frac{2\,984\,145}{653\,072}\,y_3^3 + \frac{14\,580}{5831}\sqrt{2}y_4^3 + \frac{3125}{10\,976}\,y_1^2y_2 - \frac{2\,442\,681}{268\,912}\,y_1^2y_3 + \frac{5625}{2401}\sqrt{2}y_1^2y_4 + \frac{32\,815\,295}{22\,127\,616}\,y_1y_2^2 - \frac{13\,471\,055}{1\,613\,472}\,y_2^2y_3 + \frac{2250}{2401}\sqrt{2}y_2^2y_4 - \frac{3\,334\,573}{614\,656}\,y_1y_3^2 + \frac{18\,225}{5831}\sqrt{2}y_3^2y_4 + \frac{17\,067}{5488}\,y_1y_4^2 + \frac{2025}{1372}\,y_2y_4^2 - \frac{7\,697\,901}{2\,612\,288}\,y_3y_4^2 - \frac{2250}{2401}\,y_1y_2y_3 + \frac{7\,008\,563}{1\,613\,472}\sqrt{2}y_1y_2y_4 + \frac{6075}{2744}\sqrt{2}y_1y_3y_4 - \frac{2\,411\,799}{1\,229\,312}\sqrt{2}y_2y_3y_4, \tag{B5}$$

$$x_2 = y_2 + \left(\frac{11}{14}\mu_1 - \frac{75}{112}\mu_2\right)y_1 - \left(\frac{33}{14}\mu_1 - \frac{135}{28}\mu_2\right)y_3 + \frac{3125}{32\,928}y_1^3 + \frac{18\,077\,035}{22\,127\,616}y_2^3$$
$$-\frac{15\,795}{5831}y_3^3 - \frac{10\,523\,687}{5\,224\,576}\sqrt{2}y_4^3 - \frac{2\,279\,897}{22\,127\,616}y_1^2y_2 - \frac{1125}{2401}y_1^2y_3$$
$$-\frac{10\,239\,809}{1\,613\,472}\sqrt{2}y_1^2y_4 + \frac{1875}{10\,976}y_1y_2^2 - \frac{6750}{2401}y_2^2y_3 - \frac{7\,647\,523}{3\,226\,944}\sqrt{2}y_2^2y_4$$
$$+\frac{1\,430\,797}{614\,656}y_2y_3^2 - \frac{2\,984\,145}{1\,306\,144}\sqrt{2}y_3^2y_4 + \frac{2025}{1372}y_1y_4^2 - \frac{69}{5488}y_2y_4^2$$
$$-\frac{14\,580}{5831}y_3y_4^2 + \frac{1\,455\,883}{403\,368}y_1y_2y_3 + \frac{4500}{2401}\sqrt{2}y_1y_2y_4 - \frac{3\,342\,301}{1\,229\,312}\sqrt{2}y_1y_3y_4$$
$$-\frac{2025}{2744}\sqrt{2}y_2y_3y_4, \tag{B6}$$

$$x_3 = y_3 + \left(\frac{74}{21}\mu_1 - \frac{265}{84}\mu_2\right)y_2 - \sqrt{2}\left(\frac{37}{112}\mu_1 + \frac{159}{224}\mu_2\right)y_4 - \frac{13\,083\,179}{7\,260\,624}y_1^3$$
$$+\frac{13\,250}{21\,609}y_2^3 + \frac{10\,816\,397}{9\,834\,496}y_3^3 - \frac{4293}{21\,952}\sqrt{2}y_4^3 + \frac{6625}{21\,609}y_1^2y_2$$
$$+\frac{31\,624\,067}{11\,063\,808}y_1^2y_3 - \frac{3975}{5488}\sqrt{2}y_1^2y_4 - \frac{79\,685\,939}{14\,521\,248}y_1y_2^2 - \frac{1\,177\,091}{3\,687\,936}y_2^2y_3$$
$$+\frac{1325}{5488}\sqrt{2}y_2^2y_4 + \frac{4\,250\,405}{1\,959\,216}y_1y_3^2 + \frac{31\,005}{5831}y_2y_3^2 - \frac{21\,465}{21\,952}\sqrt{2}y_3^2y_4$$
$$-\frac{101\,239\,255}{7\,836\,864}y_1y_4^2 + \frac{9540}{5831}y_2y_4^2 - \frac{8\,645\,183}{9\,834\,496}y_3y_4^2 - \frac{5475}{1372}\sqrt{2}y_1y_2y_4$$
$$-\frac{23\,850}{5831}\sqrt{2}y_1y_3y_4 + \frac{21\,906\,895}{3\,918\,432}\sqrt{2}y_2y_3y_4, \tag{B7}$$

$$x_4 = y_4 - \sqrt{2}\left(\frac{74}{21}\mu_1 - \frac{265}{84}\mu_2\right)y_1 - \sqrt{2}\left(\frac{37}{112}\mu_1 - \frac{159}{224}\mu_2\right)y_3 - \frac{33\,125}{64\,827}\sqrt{2}y_1^3$$
$$-\frac{132\,018\,655}{43\,563\,744}\sqrt{2}y_2^3 - \frac{7155}{21\,952}\sqrt{2}y_3^3 - \frac{22\,718\,401}{29\,503\,488}y_4^3$$
$$-\frac{13\,083\,179}{7\,260\,624}\sqrt{2}y_1^2y_2 - \frac{3975}{5488}\sqrt{2}y_1^2y_3 + \frac{12\,526\,333}{11\,063\,808}y_1^2y_4$$
$$-\frac{13\,250}{21\,609}\sqrt{2}y_1y_2^2 + \frac{1325}{5488}\sqrt{2}y_2^2y_3 - \frac{13\,539\,709}{3\,687\,936}y_2^2y_4 - \frac{11\,925}{5831}\sqrt{2}y_1y_3^2$$
$$-\frac{15\,770\,705}{1\,959\,216}\sqrt{2}y_2y_3^2 - \frac{1\,085\,607}{9\,834\,496}y_3^2y_4 - \frac{28\,620}{5831}\sqrt{2}y_1y_4^2$$
$$-\frac{7\,051\,605}{2\,612\,288}\sqrt{2}y_2y_4^2 - \frac{12\,879}{21\,952}\sqrt{2}y_3y_4^2 - \frac{2\,248\,765}{2\,765\,952}\sqrt{2}y_1y_2y_3$$
$$-\frac{1325}{686}y_1y_2y_4 + \frac{10\,010\,555}{979\,608}y_1y_3y_4 + \frac{19\,080}{5831}y_2y_3y_4. \tag{B8}$$

The non-linear transformations for the case of two pairs of purely imaginary eigenvalues (1:1 resonance) between the co-ordinates x_i and the normal form co-ordinates y_i are given below.

$$x_1 = y_1 - \frac{1}{16}\mu_1 y_2 + \frac{5}{8}\mu_2 y_3 + \frac{255}{16}y_1^3 + \frac{205}{32}y_2^3 + \frac{205}{32}y_2^3 - \frac{7693}{384}y_4^3 + \frac{105}{32}y_1^2 y_2$$
$$-\frac{16\,785}{64}y_1^2 y_3 - \frac{1177}{32}y_1^2 y_4 + \frac{243}{16}y_1 y_2^2 + \frac{16\,785}{64}y_2^2 y_3 + \frac{345}{32}y_2^2 y_4$$
$$-\frac{1623}{128}y_1 y_3^2 + \frac{45}{256}y_2 y_3^2 + \frac{1613}{128}y_3^2 y_4 + \frac{4503}{128}y_1 y_4^2 - \frac{1005}{256}y_2 y_4^2$$
$$+\frac{12\,495}{128}y_3 y_4^2 + \frac{615}{16}y_1 y_2 y_3 - \frac{16\,815}{32}y_1 y_2 y_4 + \frac{45}{128}y_1 y_3 y_4$$
$$-\frac{1321}{64}y_2 y_3 y_4, \tag{B9}$$

$$x_2 = y_2 - \frac{1}{16}\mu_1 y_1 - \frac{5}{8}\mu_2 y_4 - \frac{45}{32}y_1^3 + \frac{159}{16}y_2^3 - \frac{1681}{128}y_3^3 - \frac{27\,045}{128}y_4^3 + \frac{115}{16}y_1^2 y_2$$
$$-\frac{985}{32}y_1^2 y_3 + \frac{17\,265}{64}y_1^2 y_4 - \frac{105}{32}y_1 y_2^2 + \frac{153}{32}y_2^2 y_3 - \frac{17\,265}{64}y_2^2 y_4 - \frac{915}{256}y_1 y_3^2$$
$$-\frac{3433}{128}y_2 y_3^2 - \frac{32\,625}{128}y_3^2 y_4 - \frac{45}{256}y_1 y_4^2 + \frac{553}{128}y_2 y_4^2 - \frac{1037}{128}y_3 y_4^2$$
$$-\frac{17\,295}{32}y_1 y_2 y_3 - \frac{391}{16}y_1 y_2 y_4 + \frac{2391}{64}y_1 y_3 y_4 - \frac{45}{128}y_2 y_3 y_4, \tag{B10}$$

$$x_3 = y_3 - \frac{1}{8}\mu_1 y_1 - \left(\frac{1}{16}\mu_1 + \frac{5}{4}\mu_2\right)y_4 + \frac{15}{8}y_1^3 - \frac{21}{4}y_2^3 - \frac{1691}{128}y_3^3 - \frac{80\,085}{256}y_4^3$$
$$-\frac{41}{4}y_1^2 y_2 + \frac{299}{16}y_1^2 y_3 + \frac{315}{32}y_1^2 y_4 + \frac{75}{8}y_1 y_2^2 - \frac{123}{16}y_2^2 y_3 + \frac{405}{32}y_2^2 y_4$$
$$-\frac{33\,765}{64}y_1 y_3^2 + \frac{117}{32}y_2 y_3^2 - \frac{217\,665}{256}y_3^2 y_4 - \frac{33\,915}{64}y_1 y_4^2 + \frac{363}{32}y_2 y_4^2$$
$$-\frac{10\,095}{128}y_3 y_4^2 - \frac{165}{16}y_1 y_2 y_3 + \frac{501}{8}y_1 y_2 y_4 + \frac{1237}{16}y_1 y_3 y_4$$
$$-\frac{315}{32}y_2 y_3 y_4, \tag{B11}$$

$$x_4 = y_4 + \frac{1}{8}\mu_1 y_2 - \left(\frac{1}{16}\mu_1 + \frac{1}{4}\mu_2\right)y_3 + \frac{23}{12}y_1^3 - \frac{25}{8}y_2^3 - \frac{10\,795}{256}y_3^3 - \frac{2897}{384}y_4^3$$
$$-\frac{45}{8}y_1^2y_2 - \frac{405}{32}y_1^2y_3 + \frac{101}{16}y_1^2y_4 + \frac{1}{4}y_1y_2^2 + \frac{165}{32}y_2^2y_3 + \frac{683}{16}y_2^2y_4$$
$$-\frac{1227}{32}y_1y_3^2 - \frac{34\,395}{64}y_2y_3^2 + \frac{3217}{128}y_3^2y_4 - \frac{917}{32}y_1y_4^2 - \frac{34\,245}{64}y_2y_4^2$$
$$-\frac{56\,895}{256}y_3y_4^2 + \frac{181}{8}y_1y_2y_3 - \frac{315}{16}y_1y_2y_4 + \frac{165}{32}y_1y_3y_4$$
$$+\frac{363}{16}y_2y_3y_4. \tag{B12}$$